

Synthesis of Novel Hybrid Quinolino[4,3- b][1,5]Naphthyridines and Quinolino[4,3- b][1,5]Naphthyridin-6(5H)-one Derivatives and Biological Evaluation as Topoisomerase I Inhibitors and Antiproliferatives.

*Endika Martín-Encinas,^a Asier Selas,^{a,b} Cinzia Tesauro,^b Gloria Rubiales,^a Birgitta R. Knudsen,^b
Francisco Palacios^{a,*} and Concepción Alonso^{a,*}*

^a Departamento de Química Orgánica I, Facultad de Farmacia and Centro de Investigación Lascaray (Lascaray Research Center). Universidad del País Vasco/Euskal Herriko Unibertsitatea (UPV/EHU). Paseo de la Universidad 7, 01006 Vitoria-Gasteiz, Spain.

^b Department of Molecular Biology and Genetics and Interdisciplinary Nanoscience Center (iNANO), Aarhus University, Aarhus 8000, Denmark.

Keywords: Quinolino[4,3-*b*][1,5]naphthyridines, quinolino[4,3-*b*][1,5]naphthyridin-6-ones, topoisomerase I, enzyme inhibition, topoisomerase I poison, antiproliferative effect

Abbreviations: CCK8, cell counting kit; CPT, camptothecin; CPTs, camptothecin derivatives; HDAr, hetero-Diels-Alder reaction; SDS, sodium dodecyl sulfate; TopI, topoisomerase I; TLC, thin layer chromatography.

ABSTRACT. The topoisomerase I enzymatic inhibition of hybrid quinolino[4,3-*b*][1,5]naphthyridines and quinolino[4,3-*b*][1,5]naphthyridin-6(5*H*)-ones was investigated. First, the synthesis of these fused compounds was performed by intramolecular [4+2]-cycloaddition reaction of functionalized aldimines obtained by the condensation of 3-aminopyridine and unsaturated aldehydes affording corresponding hybrid 5-tosylhexahydroquinolino[4,3-*b*][1,5]naphthyridine and tetrahydroquinolino[4,3-*b*][1,5]naphthyridin-6(5*H*)-one compounds with good to high general yields. Subsequent dehydrogenation led to the corresponding more unsaturated dihydro[1,5]naphthyridine and [1,5]naphthyridin-6(5*H*)-one derivatives in quantitative yields. The new polycyclic products show excellent-good activity as topoisomerase I (TopI) inhibitors that lead to TopI induced nicking of plasmids. This is consistent with the compounds acting as TopI poisons resulting in the accumulation of trapped cleavage complexes in the DNA. The cytotoxic effect on cell lines A549, SKOV3 and on non-cancerous MRC5 was also screened. Tetrahydroquinolino[4,3-*b*][1,5]naphthyridin-6(5*H*)-one **9** resulted the most cytotoxic compound with IC₅₀ values of 3.25±0.91 μM and 2.08±1.89 μM against the A549 cell line and the SKOV3 cell line, respectively. Also, hexahydroquinolino[4,3-*b*][1,5]naphthyridine **8a** and dihydroquinolino[4,3-*b*][1,5]naphthyridine **10a** showed good cytotoxicity against these cell lines. None of the compounds presented cytotoxic effects against non-malignant pulmonary fibroblasts (MRC-5).

1. Introduction

Cancer is one of the diseases that causes more deaths annually in the world, and because of this, the development of new anti-cancer drugs has been studied for many years [1]. It is known that topoisomerase I (TopI), an enzyme overexpressed in cancerous cells, reduces superhelical stress as well as other topological consequences generated in the separation of DNA strands in metabolic processes such as replication, transcription and recombination [2]. Due to this, TopI could represent an effective target for cancer therapy.

In this sense, many TopI inhibitors are the basis of some chemotherapeutical combinations widely used in a broad spectrum of tumors [3]. Among inhibitors, camptothecin I (CPT, Figure 1) and its derivatives are some of the most studied drugs as inhibitors of TopI, commonly used in the treatment of colon, ovarian and small-cell lung cancers [4]. However, these heterocycles present some disadvantages, such as, for example, serious side effects and structural instability due to the opening of the lactone ring at physiological pH [5].

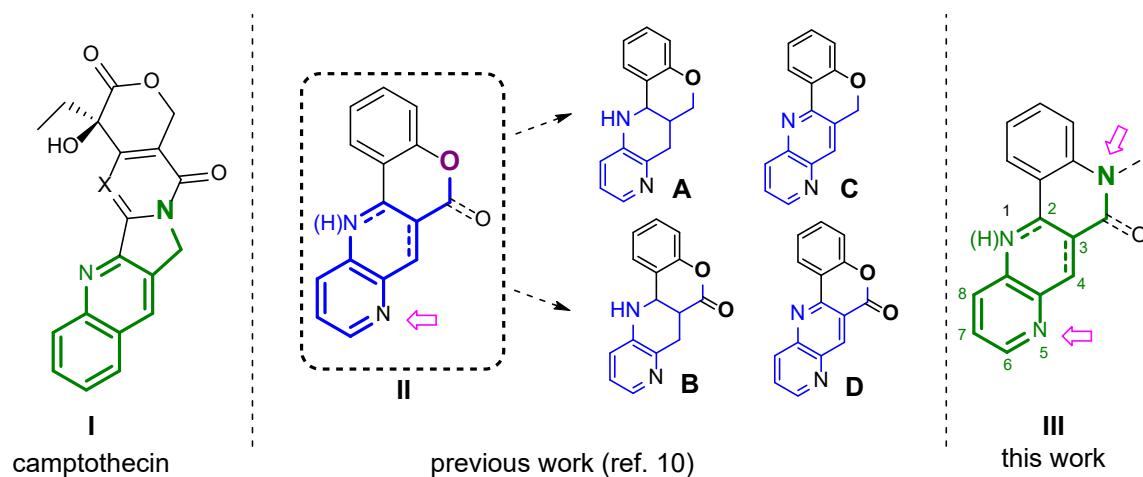


Figure 1. Structures of camptothecin I, chromeno[4,3-*b*][1,5]naphthyridine derivatives II (A, B, C and D)¹⁰ and novel quinolino[4,3-*b*][1,5]naphthyridine derivatives III.

From a chemical structural point of view, camptothecin and its derivatives present an angularly fused pentacyclic structure which, according to the proposed TopI inhibition mechanism as poison, seems to be relevant in improving the π - π stacking interactions with the DNA base pairs and consequently in avoiding the completion of the enzymatic reaction of TopI [2]. Taking into account the structural features of camptothecin, our group developed the synthesis and the biological studies of quinolinic derivatives,[6] which demonstrated to be good TopI inhibitors, antiproliferative and antileishmanial agents [7]. Likewise, 1,5-naphthyridines, with an additional nitrogen atom in the quinolinic core of the CPTs, showed good inhibitory activity against *Leishmanial* TopI (LTopI) enzyme [8] and 1,5-naphthyridines fused with a carbocycle structure (indene) showed good TopI inhibition with antileishmanial and antiproliferative activity [9]. More recently we developed the synthesis of chromeno[4,3-*b*][1,5]naphthyridine derivatives **II** (Figure 1) which showed a moderate inhibitory activity of TopI as well as moderate cytotoxicity against cancerous cells [10].

Bearing all this in mind, we hypothesized that hybrid quinolino[4,3-*b*][1,5]naphthyridine derivatives **III** (Figure 1) would present improved TopI inhibitory and antiproliferative cytotoxic properties compared to other biologically active structures **II**. We suspected that the isosteric replacement of the oxygen atom present in the structure of chromeno[4,3-*b*][1,5]naphthyridine derivatives **II** (Figure 1) by a nitrogen atom, as appears in the structure core of compounds **III** (Figure 1), would afford heterocycles with increased biological activity as TopI inhibitors. In addition, this structural change from an oxygen atom to a nitrogen atom would give rise to condensed heterocycles not described until today.

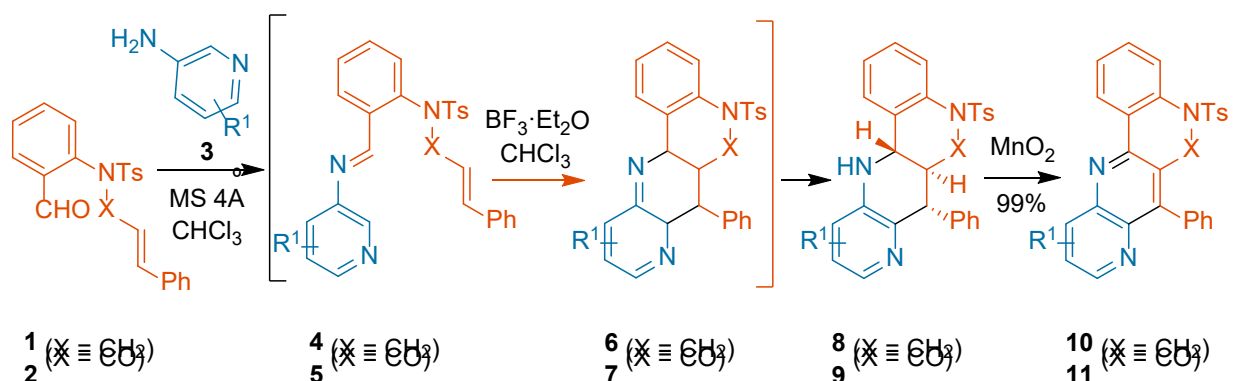
The most suitable strategy for the synthesis of nitrogenated chemical compounds, such as naphthyridines, would be the hetero-Diels-Alder reaction (HDAr),[11] a highly atom-economic

tool that presents interesting applications [12]. In fact, among them, the Povarov reaction may represent a direct route to naphthyridine derivatives [13]. Furthermore, in the search of a methodology for the preparation of molecules with higher molecular diversity, intramolecular Povarov reaction could be considered as an important strategy for the synthesis of several ring-fused derivatives by a single operation [14].

In this work we report the straightforward synthesis of quinolino[4,3-*b*][1,5]naphthyridine derivatives **III** (Figure 1) by intramolecular Povarov reaction. The preparation of these new families of compounds represents an interesting challenge in organic chemistry, due to the potential interest of these molecules not only in synthetic but also in medicinal chemistry.

2. Chemistry

The hybrid substituted quinolino[4,3-*b*][1,5]naphthyridine derivatives **III** (Figure 1) were synthesized by an intramolecular Povarov [4+2]-cycloaddition reaction. First, we started with the preparation of 5-tosyl functionalized aldehydes **1** and **2** (Scheme 1, X = CH₂, CO) which tailored a double bond in their structure as indicated.



Scheme 1. Syntheses of quinolino[4,3-*b*][1,5]naphthyridine derivatives **8/10** and quinolino[4,3-*b*][1,5]naphthyridin-6(5*H*)-one derivatives **9/11**.

Afterwards, we carried out the preparation *in situ* of functionalized aldimines **4** and **5**, by condensation between 3-aminopyridine **3** and corresponding functionalized aldehydes **1** or **2**, followed with their intramolecular cyclization in refluxing chloroform in the presence of Lewis acid as $\text{BF}_3 \cdot \text{Et}_2\text{O}$ (Scheme 1).

For the formation of compounds **8** and **9** the addition of two equivalents of $\text{BF}_3 \cdot \text{Et}_2\text{O}$ was necessary. In this sense, the corresponding tetracyclic *endo*-5-tosyl-5,6,6a,7,12,12a-hexahydroquinolino[4,3-*b*][1,5]naphthyridines **8** ($\text{X} = \text{CH}_2$) or *endo*-5-tosyl-6a,7,12,12a-tetrahydroquinolino[4,3-*b*][1,5]naphthyridin-6(5*H*)-one **9** ($\text{X} = \text{CO}$) were selectively obtained with good yields (70-95%, Scheme 1, Chart 1) in a regio- and stereospecific way. Unfortunately, with the exception of compound **9** ($\text{R}^1 = \text{H}$), the *endo*-5-tosyl-6a,7,12,12a-tetrahydroquinolino[4,3-*b*][1,5]naphthyridin-6(5*H*)-ones were unstable maybe by the instability of the lactam group under the purification conditions.

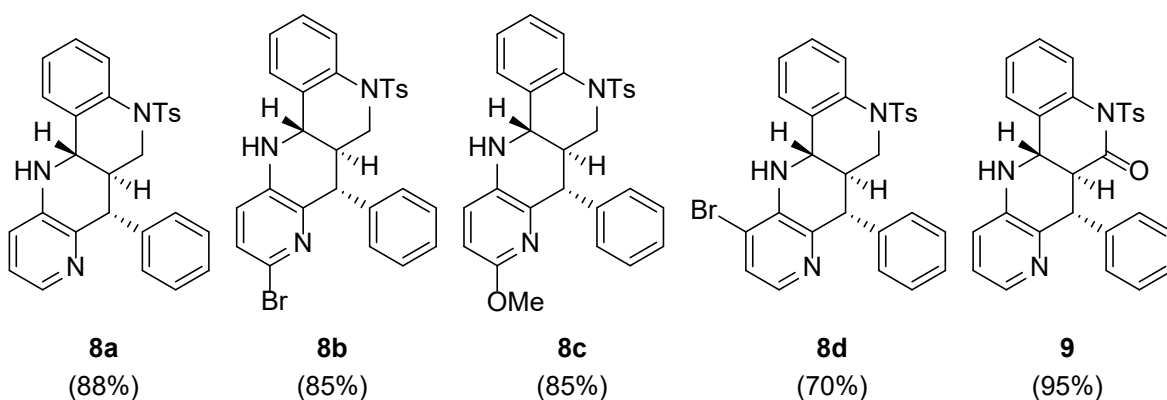


Chart 1. Structures of *endo*-5-tosyl-5,6,6a,7,12,12a-hexahydroquinolino[4,3-*b*][1,5]naphthyridines **8** and *endo*-5-tosyl-6a,7,12,12a-tetrahydroquinolino[4,3-*b*][1,5]naphthyridin-6(5*H*)-one **9** obtained by intramolecular Povarov reaction.

Formation of *endo*-5-tosyl-5,6,6a,7,12,12a-hexahydroquinolino[4,3-*b*][1,5]naphthyridine derivatives **8** and *endo*-5-tosyl-6a,7,12,12a-tetrahydroquinolino[4,3-*b*][1,5]naphthyridin-6(5*H*)-

one derivatives **9** may be explained by a regio- and stereospecific intramolecular [4+2]-cycloaddition reaction of aldimines **4/5** to give intermediates **6/7** followed by prototropic tautomerization.

The methodology tolerates a wide range of electron-releasing and electron-withdrawing substituents in the starting 3-aminopyridine **3**. It is noteworthy that this methodology allowed the preparation of adducts with methoxy groups ($R^1 = \text{OMe}$), since in previous studies of our group it has been suggested that this substituent may improve the biological activity of heterocyclic compounds.^{7,8} As far as we know, this strategy represents the first example for the preparation of 5,6,6a,7,12,12a-hexahydroquinolino[4,3-*b*][1,5]naphthyridines **8** and 6a,7,12,12a-tetrahydroquinolino[4,3-*b*][1,5]naphthyridin-6(*5H*)-one **9**.

Subsequent dehydrogenation of 5-tosylhexahydroquinolino[4,3-*b*][1,5]naphthyridines **8** ($X = \text{CH}_2$) and 5-tosyltetrahydroquinolino[4,3-*b*][1,5]naphthyridin-6(*5H*)-one **9** ($X = \text{CO}$) under the reaction conditions would afford 5-tosyldihydroquinolino[4,3-*b*][1,5]naphthyridines **10** ($X = \text{CH}_2$) and 5-tosylquinolino[4,3-*b*][1,5]naphthyridin-6(*5H*)-one **11** ($X = \text{CO}$), respectively, in quantitative yields (Scheme 1, Chart 2). This dehydrogenation reaction was performed with 4 equivalents of MnO_2 in toluene at 111°C for 48h as previously reported [15].

The preparation of 5-tosyldihydroquinolino[4,3-*b*][1,5]naphthyridines **10** in a single step may be also performed. When aldehyde **12**, with a triple bond in their structure, were used for the preparation of corresponding aldimines **13**, after a subsequent intramolecular cycloaddition in the presence of $\text{BF}_3 \cdot \text{Et}_2\text{O}$ the 5-tosyldihydroquinolino[4,3-*b*][1,5]naphthyridines **10** were isolated with good yields (Scheme 2, Chart 2).

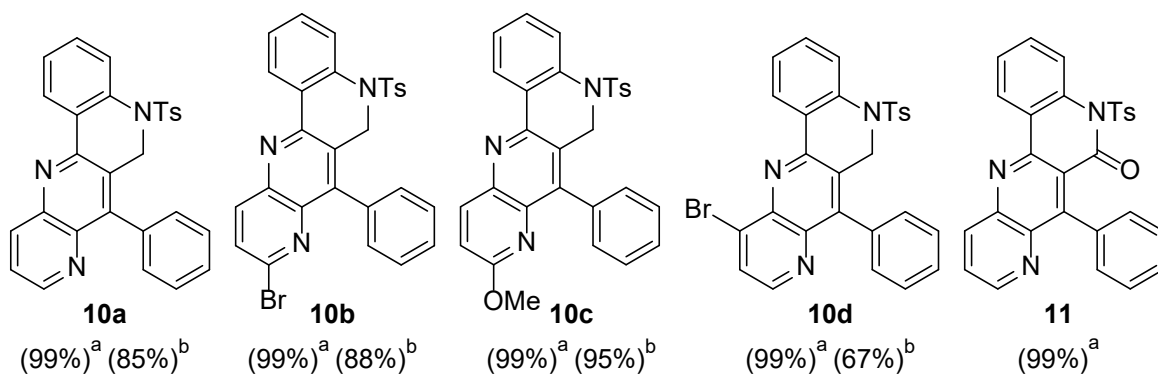
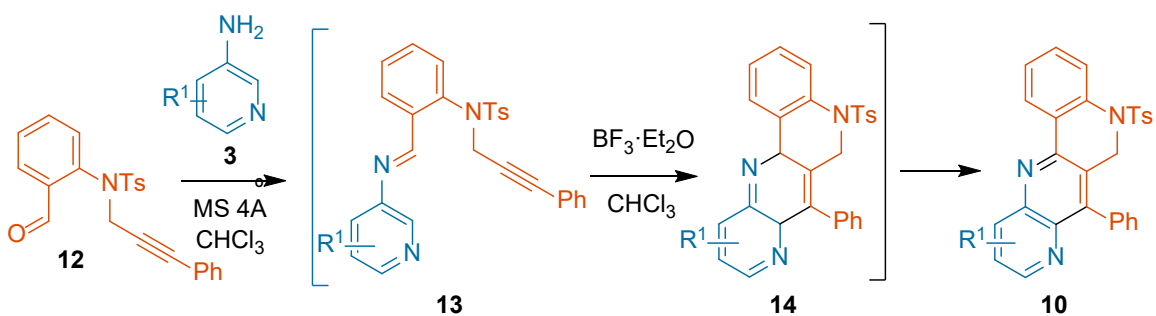


Chart 2. Structures of dihydroquinolono[4,3-*b*][1,5]naphthyridines **10** and quinolino[4,3-*b*][1,5]naphthyridin-6(5*H*)-one **11**. ^aObtained by the dehydrogenation of compounds **8** and **9**. ^bObtained by Povarov reaction of aldimines **13**.

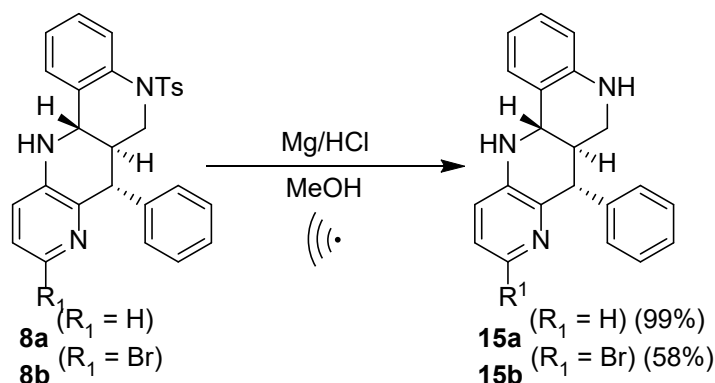
In a similar way to that reported in Scheme 1, formation of 5-tosylquinolino[4,3-*b*][1,5]naphthyridine derivatives **10** may be explained by a regioselective intramolecular [4+2]-cycloaddition reaction of aldimines **13** to give intermediates **14** followed by protodehydrogenation under the reaction conditions. It should be noted that the compounds **10** were obtained in the presence of $\text{BF}_3 \cdot \text{Et}_2\text{O}$. As far as we know, this strategy represents the first example for the direct synthesis of 5-tosyl-5,6-dihydroquinolino[4,3-*b*][1,5]naphthyridines **10**.



Scheme 2. Synthesis of quinolino[4,3-*b*][1,5]naphthyridine derivatives **10** by Povarov reaction.

With 5-tosyl-5,6-dihydroquinolino[4,3-*b*][1,5]naphthyridine derivatives **10** in hand, we wondered if the presence of the tosyl group in the structure of these adducts was essential for their

biological activity or if those derivatives without tosyl groups may present a different biological behavior. For these reasons, afterwards we performed the deprotection of the tosyl group in compounds **8a** and **8b**. The deprotection attempts were carried out under different reaction conditions such as the acid treatment with TFA or H₂SO₄, the treatment with naphthalene/Na mixture or the treatment with SiMe₂Cl and only decomposition products were obtained. However, the corresponding derivatives **15** could be isolated when the 5-tosylhexahydroquinolino[4,3-*b*][1,5]naphthyridines **8** were treated with Mg under acidic conditions (Scheme 3).



Scheme 3. Synthesis of derivatives **15** by deprotection of tosyl group with magnesium.

To sum up, in the described methodology hybrid quinolino[4,3-*b*][1,5]naphthyridine derivatives **8-11** and **15** are obtained in an efficient and straightforward way for the first time. In next steps, the biological behavior of these novel compounds as TopI inhibitors and as antiproliferative agents was studied.

3. Biological results and discussion

3.1. Inhibition of Topoisomerase I. The inhibitory effect of the synthesized derivatives on human topoisomerase I (TopI) was investigated. A conventional supercoiled plasmid relaxation assay (Figure 2) was used to determine if the newly synthesized tetracyclic *endo*-5,6,6a,7,12,12a-

hexahydroquinolino[4,3-*b*][1,5]naphthyridines **8** and **15**, *endo*-6a,7,12,12a-tetrahydroquinolino[4,3-*b*][1,5]naphthyridin-6(5*H*)-one **9**, 5,6-dihydroquinolino[4,3-*b*][1,5]naphthyridines **10** and quinolino[4,3-*b*][1,5]naphthyridin-6(5*H*)-one **11** inhibit human TopI relaxation activity that converts supercoiled plasmid DNA to relaxed DNA (Table 1). In these experiments, compound samples were mixed with supercoiled plasmid DNA substrate followed by addition of enzyme and continued incubation for increasing time intervals (15 seconds, 1 minute and 3 minutes). The reaction was terminated by the addition of SDS. DNA relaxation products were then resolved by gel electrophoresis in a 1% agarose gel and visualized by gel red staining. CPT was used as a positive control (Figure 2).

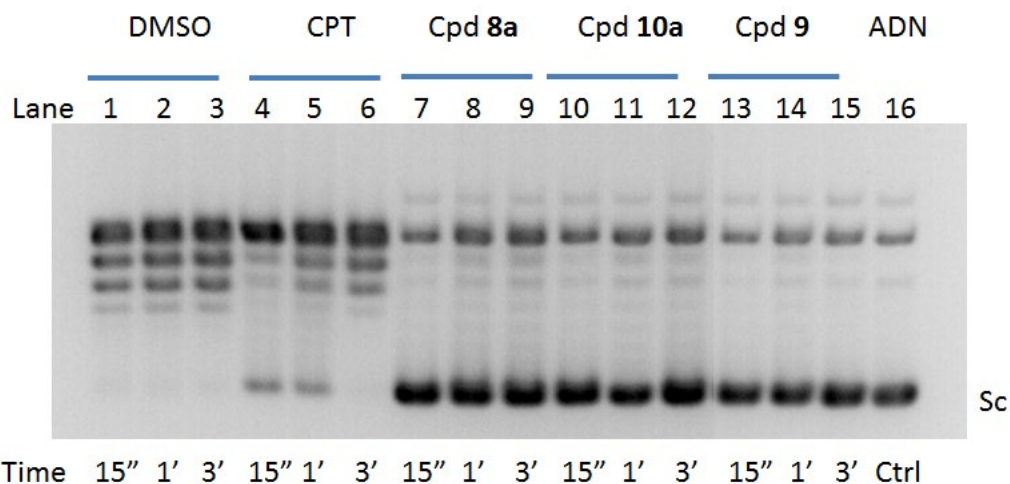


Figure 2. Inhibition of TopI activity along the time (15'', 1' and 3') by compounds **8a**, **10a**, **9** and CPT at 100 μ M: lanes 1-3, DNA+TopI+DMSO; lanes 4-6, DNA+TopI+CPT 100 μ M; lanes 7-9, DNA+TopI+**8a** 100 μ M; lanes 10-12, DNA+TopI+**10a** 100 μ M; lanes 13-15, DNA+TopI+**9** 100 μ M; lane 16, control DNA. Reaction samples were mixed with the supercoiled DNA substrate before adding enzyme at 37 $^{\circ}$ C and separated by electrophoresis on a 1% agarose gel, and then stained with gel red, and photographed under UV light as described in the TopI mediated DNA relaxation assay. Sc, supercoiled DNA.

The TopI inhibitory activity of new compounds was tested by detecting the conversion of supercoiled DNA (Sc, Figure 2) to its relaxed form in the presence of the purified enzyme with or

without added compound. The results are shown in a qualitative fashion relative to the TopI inhibitory activity of CPT (Table 1).

Table 1. TopI inhibitory activity of compounds **8**, **9**, **10**, **11** and **15**.

Entry	Compound	X	R ¹	NTs/NH	% Inhibition ^a		
					15 seconds	1 minute	3 minutes
1	Camptothecin (CPT)				++	++	-
2	8a	CH ₂	H	NTs	+++	+++	+++
3	8b	CH ₂	4-Br	NTs	++	+++	+++
4	8c	CH ₂	4-MeO	NTs	++	++	+++
5	8d	CH ₂	6-Br	NTs	+++	+++	+++
6	9	CO	H	NTs	+++	+++	+++
7	10a	CH ₂	H	NTs	+++	+++	+++
8	10b	CH ₂	4-MeO	NTs	++	++	+++
9	10c	CH ₂	4-Br	NTs	+++	+++	+++
10	10d	CH ₂	6-Br	NTs	+++	+++	+++
11	11	CO	H	NTs	+++	+++	+++
12	15a	CH ₂	H	NH	++	+++	+++
13	15b	CH ₂	4-Br	NH	+++	+++	+++

^a The activity of the compounds to inhibit TopI relaxation was expressed semiquantitatively as follows: ⊖, no activity; ++ similar activity to camptothecin; +++ strong activity.

The effects of CPT and DMSO (the solvent of CPT and the new compounds) were tested as a positive and a negative control, respectively, in the experiment. As expected CPT inhibited relaxation as more plasmid was left unrelaxed at shorter time points when 100 μM CPT was added compared to the DMSO control (compare lanes 4 and 5 with lanes 1 and 2 in Figure 2). Note, that consistent with reversible binding of CPT to the TopI cleavage complex relaxation of the plasmid was observed upon prolonged incubation (lane 6). All of the tested new compounds inhibited

relaxation considerably stronger than CPT when added to the same concentration (100 μ M) and under similar experimental conditions as no (or extremely little) conversion of supercoiled plasmid to relaxed forms could be observed in the presence of any of the new compounds in the duration of the experiment (compare lanes 7-15 with the plasmid control in lane 16).

Based on the results of the relaxation assays, all synthesized compounds present high inhibitory activity of TopI at low reaction times (15 seconds and 1 minute). Surprisingly, after 3 minutes of enzymatic reaction, all compounds, 5-tosylhexahydroquinolino[4,3-*b*][1,5]naphthyridines **8** and hexahydroquinolino[4,3-*b*][1,5]naphthyridines **15**, 5-tosyltetrahydroquinolino[4,3-*b*][1,5]naphthyridin-6(5*H*)-one **9**, 5-tosyldihydroquinolino[4,3-*b*][1,5]naphthyridines **10** and 5-tosylquinolino[4,3-*b*][1,5]naphthyridin-6(5*H*)-one **11** maintain their high TopI inhibitory activity, in all cases over 75% (Table 1 and Table S1 of Supplementary Material). Considering these results, the novel families of naphthyridines fused with quinolines and quinolinones are as effective as CPT inhibiting TopI at short enzymatic reaction time and have a more pronounced inhibitory effect than the natural inhibitor, CPT, at longer reaction times. Even so, CPT still presents better results in the theoretical study of molecular docking (*vide infra*). Therefore, the isosteric substitution of an oxygen atom present in compounds **A**, **B**, **C** and **D** (Figure 1, *vide supra*) by a NTs group or a nitrogen atom lead to an increase in the TopI inhibition for the corresponding compounds **8**, **9**, **10**, **11** and **15**.

3.2. The new compounds act as TopI poisons. In order to investigate whether quinolino[4,3-*b*][1,5]naphthyridines **8**, **10** and **15** and quinolino[4,3-*b*][1,5]naphthyridin-6(5*H*)-ones **9** and **11** could behave as TopI poisons and generate stabilized cleavage complexes *in vitro* a nicking assay was performed. Figure 3 reports the results from the nicking assay performed with Top I in the presence of **8a**, **10a** and **9**, using CPT as a reference. This assay was performed essentially as a

standard relaxation assay. However, the reaction products was analyzed in a 1% agarose gel containing EtBr. When EtBr intercalates intact double stranded plasmid DNA it introduces positive supercoils. However, if the plasmid is nicked the supercoils are rapidly relaxed and, hence, nicked plasmid run with a mobility of relaxed plasmid in the gel while supercoiled and intact relaxed plasmid run with a mobility of supercoiled plasmid in the gel. As expected, CPT stabilized the cleavage complexes generated by TopI leading to an increase in the amount of nicked plasmid DNA (Figure 3, lanes 4-6).

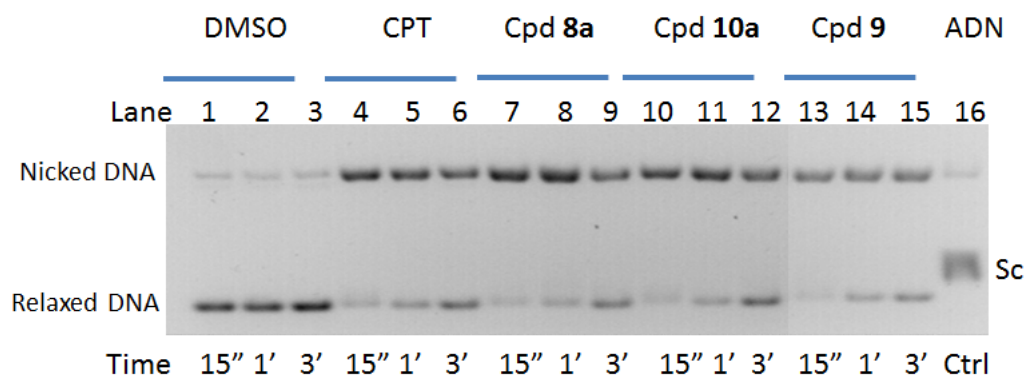


Figure 3. DNA nicking assay of TopI activity in absence (only DMSO) and presence of CPT and compounds **8a**, **10a**, **9** and CPT at 100 μ M: lanes 1-3, DNA+TopI+DMSO; lanes 4-6, DNA+TopI+CPT 100 μ M; lanes 7-9, DNA+TopI+**8a** 100 μ M; lanes 10-12, DNA+TopI+**10a** 100 μ M; lanes 13-15, DNA+TopI+**9** 100 μ M; lane 16, control DNA. Reaction samples were mixed with the supercoiled DNA substrate before adding enzyme at 37 $^{\circ}$ C and separated by electrophoresis on a 1% agarose gel with ethidium bromide, and then stained with gel red, and photographed under UV light. Sc, supercoiled DNA.

Notably, it can be observed that in the presence of **8a**, **10a** and **9** derivatives (Figure 3, lanes 7-15) nicked plasmid DNA was also generated *in vitro*. This is consistent with the drugs leading to accumulation of cleavage complexes in the plasmid. With these results in hand, then we can assume that new prepared quinolino[4,3-*b*][1,5]naphthyridines **8**, **10** and **15** and quinolino[4,3-

b][1,5]naphthyridin-6(5*H*)-ones **9** and **11** may be considered as TopI poison (Figure S1 of Supplementary Material).

To address the mechanism of inhibitions of the compounds **8a**, **10a** and **9** a classical cleavage-ligation equilibrium experiment was carried out essentially as described in literature [16]. TopI was incubated with a double stranded Cy3-labelled DNA substrate of 32bp in the presence of CPT (as a positive control) or each of the compounds or DMSO that was used a solvent of the drugs. As evident from figure 4, incubation of TopI with the DNA fragment in the presence of either CPT or the compounds resulted in the appearance of low molecular weight products (relative to the DNA substrate) corresponding to the accumulation of cleavage complexes on the DNA (the most pronounced cleavage product is marked by an asterisk). Such products were not observed in the presence of DMSO only. This is in agreement with a poison mode of action of the compounds **8a**, **10a** and **9**. The accumulation of cleavage complexes was concentration dependent (see figure 4, lanes 5-7, lanes 8-10 and lanes 11-13). Note that the new compounds were more soluble than CPT and, hence, higher concentrations of these drugs could be added. This is also confirmed by the inability of CPT to induce cleavage complexes when used at high concentration, which can most probably be ascribed to precipitation of the drug at these conditions (see figure 4 lane 4). Of the three tested drugs, compounds **8a** and **9** appeared considerably more potent in generating the major cleavage product compared to compound **10a**. However, compound **10a** appeared equally or even slightly more potent in generating the minor cleavage products with different gel-electrophoretic mobilities, which in turn may explain the induction of plasmid nicking of this compound observed in Figure 4.

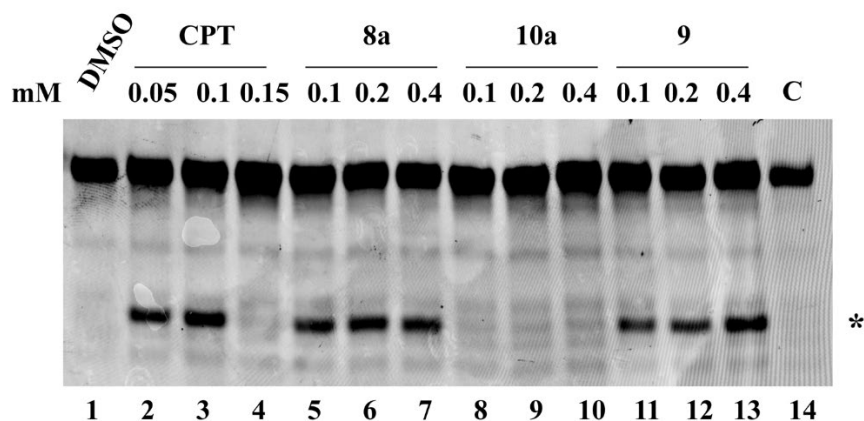


Figure 4. Gel electrophoresis of the products coming from the incubation of the wild-type topoisomerase I with the Cy3-labelled duplex DNA, in the absence (DMSO, lane 1) or presence of increasing concentrations of CPT (lanes 2-4), compound **8a** (lanes 5-7), compound **10a** (lanes 8-10) or compound **9** (lanes 11-13). C (Lane 14) shows the mobility of the DNA substrate in absence of TopI. The asterisk indicates the mobility of the major DNA cleavage product generated upon addition of drugs.

3.3. In Vitro Cytotoxicity. The cytotoxicity of the new quinolino[4,3-*b*][1,5]naphthyridines **8**, **10** and **15** and quinolino[4,3-*b*][1,5]naphthyridin-6(5*H*)-ones **9** and **11** was investigated *in vitro* by testing the antiproliferative activities against two human cancer cell lines: A549 (carcinomic human alveolar basal epithelial cell) and SKOV3 (human ovarian carcinoma). The cell counting kit (CCK8) assay was employed to assess growth inhibition and, the cell proliferation inhibitory activities of the compounds are listed in Table 2 as IC₅₀ values.

Some saturated derivatives, such as compounds **8a**, **8d** and **9** (Chart 1), demonstrated cytotoxic when evaluated in both cancerous cell lines. For instance, derivative **8a** showed IC₅₀ values of 7.25±0.81 μM and 8.08±1.39 μM against the A549 cell line and the SKOV3 cell line, respectively (Table 2, entry 2). 5-Tosyltetrahydroquinolino[4,3-*b*][1,5]naphthyridin-6(5*H*)-one **9** was the most cytotoxic drug with IC₅₀ values of 3.25±0.91 μM and 2.08±1.89 μM against the A549 cell line and the SKOV3 cell line, respectively (Table 2, entry 6). The most aromatized compounds **10** and **11**, the 5-tosyldihydroquinolino[4,3-*b*][1,5]naphthyridine **10a** (Chart 2), demonstrated IC₅₀ values of

7.34±0.17 μM and 8.65±0.57 μM against the A549 cell line and the SKOV3 cell line, respectively (Table 2, entry 7).

Table 2. Antiproliferative activity of compounds **8**, **9**, **10**, **11** and **15**.

Entry	Comp.	X	R ¹	R ²	Cytotoxicity IC ₅₀ (μM) ^a		
					lung A549	ovarian SKOV3	lung MRC-5
1	Camptothecin		(CPT)		(1.0±0.06)·10 ⁻³	(5.5±0.01)·10 ⁻³	(1.7±0.96)·10 ⁻⁵
2	8a	CH ₂	H	Ts	7.25±0.81	8.08±1.39	>50
3	8b	CH ₂	3-Br	Ts	>50	>50	>50
4	8c	CH ₂	3-MeO	Ts	>50	>50	>50
5	8d	CH ₂	5-Br	Ts	28.31±1.53	33.53±3.31	>50
6	9	CO	H	Ts	3.25±0.91	2.08±1.89	>50
7	10a	CH ₂	H	Ts	7.34±0.17	8.65±0.57	>50
8	10b	CH ₂	3-Br	Ts	>50	>50	>50
9	10c	CH ₂	3-MeO	Ts	28.99±1.35	11.03±1.47	>50
10	10d	CH ₂	5-Br	Ts	>50	>50	>50
11	11	CO	H	Ts	>50	>50	>50
12	15a	CH ₂	H	H	>50	>50	>50
13	15b	CH ₂	3-Br	H	>50	>50	>50

^aThe cytotoxicity IC₅₀ values listed are the concentrations corresponding to 50% growth inhibition.

Moreover, the effects of the new drugs on the non-malignant lung fibroblasts, MRC-5, were tested in order to study potential selective toxicity of the new compounds. Of high interest none of the synthesized 1,5-naphthyridine compounds exhibited any toxicity toward MRC-5 cells (Table 2). CPT, on the other hand, exhibited cytotoxic activity against this non-cancerous cell line.

4. Computational analysis

As experimental observations indicated, the tetracyclic core of these novel compounds may be the determinant for the high TopI inhibition. Next, we performed theoretical calculations of Molecular Electrostatic Potential Surface (MEPS), HOMO-LUMO energy gap and related parameters. Therefore, we used theoretical studies using Density Functional Theory (DFT) [17] with Becke three-parameter Lee-Yang-Parr function (B3LYP) [18] and 6-31G (d, p) level of theory for the synthesized compounds to depict the potential kinetic stability and reactivity of the target compounds. [19]

4.1. Stereoelectronic properties. First, the molecular DFT-based parameters such as electronic chemical potential (μ), chemical hardness (η), global electrophilicity (ω), maximum number of accepted electrons (ΔN_{\max}) and free energy in gas and in aqueous medium for compounds **8**, **9**, **10**, **11** and **15** were calculated (Table 3).

In such a way, 5-tosyl-5,6,6a,7,12,12a-hexahydroquinolino[4,3-*b*][1,5]naphthyridine derivatives **8** and 5-tosyl-6a,7,12,12a-tetrahydroquinolino[4,3-*b*][1,5]naphthyridin-6(5*H*)-one derivative **9**, which present a tosyl (Ts) group in position 5, are more stable with gap values of 4.22 to 4.65 (Table 3, entries 2-6) than the corresponding more aromatic compounds with Ts group **10a-d** and **11** with gap values from 3.84 to 4.26 (Table 3, entries 7-11). Compound **11** is the most reactive, with a gap value of 3.84 close to the CPT (Table 3, entry 11). Moreover, compounds **8a-d** and **9** have higher chemical potential and are less electrophilic than the more aromatic derivatives **10a-d** and **11**. In fact, compound **11** is the most electrophilic compound showing a similar electrophilicity than CPT. In addition, the dipole moment of **8a-d** and **9** is greater than that of the

corresponding more aromatic compounds **10a-d** and **11** and, on the other hand, **8a-d** and **9** are less polarizable than **10a-d** and **11**.

Although all the compounds present an excellent inhibition of TopI, it is observed experimentally that the compounds **8c** and **10b**, with a methoxy group in the position 9, present the lowest values of inhibition (Table 1, entries 4 and 8). Precisely these compounds are the least electrophilic and have the highest values of chemical potential of compounds **8** and **10** respectively (Table 3).

With respect to 5,6,6a,7,12,12a-hexahydroquinolino[4,3-*b*][1,5]naphthyridines **15a,b**, without tosyl substituent at 5 position, we could say that these would be less reactive than compounds **8**, **9**, **10** and **11** of the former group. These compounds **15a,b** present the highest gap values, 4.78 and 4.55, respectively, with higher chemical potential, lower electrophilicity, lower dipole moment and polarizability than compounds of the former group with Ts substituents (Table 3, entries 12 and 13).

In general, all compounds presented in this work show values of gap, electrophilicity, chemical potential among those observed for tetrahydrochromeno[4,3-*b*][1,5]naphthyridines and chromeno[4,3-*b*][1,5]naphthyridines previously described [10]. In addition, in general, these compounds present dipolar moments much higher than tetrahydrochromeno[4,3-*b*][1,5]naphthyridines **A** and **B** (Figure 1) and chromeno[4,3-*b*][1,5]naphthyridines **C** and **D** (Figure 1) previously described [10]. These factors could indicate a different behaviour of the two types of compounds with respect to their interaction with the target.

Table 3. Calculated energies and molecular properties computed at B3LYP/6-311G** basis set level of theory for CPT and compounds **8**, **9**, **10**, **11** and **15**.

Entry	Compound	ΔG (g) (in a.u.)	ΔG (aq) (in a.u.)	E_{HOMO} (in a.u.)	E_{LUMO} (in a.u.)	Gap (-eV)	η (in a.u.)	μ (in a.u.)	ω (eV)	ΔN_{max} (in a.u.)	Dipole moment (debye)	Polarizability
1	CPT	-1182.2	-1182.2	-0.22711	-0.0929	3.65	0.13426	-0.15998	0.095314	1.191569	6.419	265.418
2	8a	-1794.8	-1794.8	-0.21287	-0.04820	4.48	0.16467	-0.13054	0.051738	0.79271	5.314	346.125
3	8b	-1909.3	-1909.4	-0.20320	-0.04817	4.22	0.15503	-0.12569	0.050947	0.81071	4.911	363.456
4	8c	-4368.4	-4368.4	-0.21786	-0.05097	4.54	0.16689	-0.13442	0.054130	0.80541	7.563	368.273
5	8d	-4368.4	-4368.4	-0.21552	-0.04961	4.51	0.16591	-0.13257	0.052962	0.79902	5.709	365.721
6	9	-1868.9	-1868.9	-0.22815	-0.05736	4.65	0.17079	-0.14276	0.059661	0.83585	5.333	343.447
7	10a	-1792.5	-1792.5	-0.23383	-0.07733	4.26	0.15650	-0.15558	0.077333	0.99412	4.802	367.601
8	10b	-1907.0	-1907.0	-0.22183	-0.07215	4.07	0.14968	-0.14699	0.072174	0.98203	3.570	393.386
9	10c	-4366.0	-4366.0	-0.23682	-0.08429	4.15	0.15253	-0.16056	0.084501	1.05261	6.944	394.390
10	10d	-4366.0	-4366.0	-0.23671	-0.08451	4.14	0.1522	-0.16061	0.084742	1.05526	5.267	387.671
11	11	-1866.5	-1866.5	-0.23631	-0.09507	3.84	0.14124	-0.16569	0.097186	1.17311	4.505	375.001
12	15a	-975.9	-975.9	-0.20211	-0.0263	4.78	0.17581	-0.11421	0.037093	0.64959	1.721	244.486
13	15b	-3549.4	-3549.4	-0.20658	-0.03944	4.55	0.16714	-0.12301	0.045266	0.73597	4.023	265.885

Abbreviations: ΔG (g): Free energy in gas phase^[a]; ΔG (aq): Free energy in aqueous medium^[b]; Gap: $E_{\text{HOMO}} - E_{\text{LUMO}}$; η : Hardness^[c]; μ : Chemical Potentials^[c]; ω : Global Electrophilicities^[c] and ΔN_{max} : Maximum Number of Accepted Electrons^[c].

^[a] Computed a B3LYP/6-311G**+ Δ ZPVE level; ^[b] Computed a B3LYP(PCM)/6-311G**+ Δ ZPVE level using water as solvent; ^[c] Computed at the B3LYP/6-311G** level of theory according to the approach and equations described previously [14].

4.2 Molecular Electrostatic Potential Surface (MEPS) analysis. The MEPS of CPT, 5-tosyl-5,6,6a,7,12,12a-hexahydroquinolino[4,3-*b*][1,5]naphthyridine derivatives **8** and 5-tosyl-6a,7,12,12a-tetrahydroquinolino[4,3-*b*][1,5]naphthyridin-6(5*H*)-one **9** (Figure S2 in Supporting Material) and the MEPS of 5-tosyl-5,6-dihydroquinolino[4,3-*b*][1,5]naphthyridines **10**, 5-tosylquinolino[4,3-*b*][1,5]naphthyridin-6(5*H*)-one **11** and hexahydroquinolino[4,3-*b*][1,5]naphthyridines **15** (Figure S3 in Supporting Material) were calculated using DFT [17] with the standard basis set B3LYP / 6-31G (d, p) level of theory.

From these calculations, it can be seen in Figures S2 and S3 that compounds **8** and **10** have the most negative local electrostatic potential over the oxygen atoms of the tosyl group and a local negative electrostatic potential over the nitrogen atom at position 8 of the tetracyclic ring system. Moreover, the most positive local electrostatic potential is located over the hydrogens of the methyl group of tosyl substituent. In the case of compound **9**, which present a carbonyl group in position 6, an additional negative potential also appears over the oxygen atom of this carbonyl group.

In contrast, for the previously reported chromenonaphthyridine derivatives **A**, **B**, **C** and **D** [10] (Figure 1) the most negative potential was located over the nitrogen atom of position 8, and the most positive potential was located over the hydrogen in the NH group at 12 position and over the hydrogens of positions 9, 10 and 11 of the tetracyclic ring system. This suggests that the interactions with the target are different in the case of quinolinonaphthyridine derivatives and probably the replacement of an oxygen by the *N*-Tosyl group is more favourable for the formation of the ligand–TopI–DNA ternary complex.

On the other hand, for compounds **15a,b**, without a tosyl group, a particular electrostatic potential map is observed (Scheme 3, Figure S3 in Supporting Material). In this case, the

positioning of local positive electrostatic potential has varied from place, being situated on the hydrogen atom of the NH group located at position 5 of the tetracyclic ring system.

4.3 Docking studies. In order to explore if our hypothesis about the isosteric substitution of the oxygen atom of chromenonaphthyridines **II** (Figure 1) by a nitrogen atom in quinolinonaphthyridines **8**, **11** and **15** may improve the enzymatic inhibition of TopI, a molecular docking study was carried out to investigate its plausible binding pattern and its interaction with the key amino acids and DNA nucleobases in the active site of the TopI. The model was derived by docking of 5-tosyl-5,6,6a,7,12,12a-hexahydroquinolino[4,3-*b*][1,5]naphthyridine derivatives **8**, 5-tosyl-6a,7,12,12a-tetrahydroquinolino[4,3-*b*][1,5]naphthyridin-6(*5H*)-one derivative **9**, 5-tosyl-5,6-dihydroquinolino[4,3-*b*][1,5]naphthyridines **10** and 5-tosylquinolino[4,3-*b*][1,5]naphthyridin-6(*5H*)-one **11** in the camptothecin binding site of the camptothecin–TopI–DNA ternary complex (PDB ID: 1T8I) [20].

The most important evaluation criterion was the observation of whether the ligands were located between C112-TGP11 and A113-T10 nucleobases, where the DNA rupture site is located, avoiding the re-ligation of such bases, according to the concept of interfacial inhibition proposed by Pommier [2]. The formation of hydrogen bonds with important residues [21] and the existence of hydrophobic interactions with TopI residues and DNA were also taken into account.

Likewise, based on the above interactions, the obtained values from the gscore parameters indicate the virtual affinity of the ligands to the complex, and gemodel, which is the theoretical value of the interaction energy of the ligand with the TopI/DNA complex, were considered (see Table 4).

Table 4. gscore and gemodel values for compounds **8**, **9**, **10** and **11** TopI inhibitors and camptothecin.

Entry	Compound	gscore (kcal/mol)	gemodel (kcal/mol)
1	8a	- 6.0	- 81.4
2	8b	- 6.2	- 78.6
3	8d	- 6.0	- 80.7
4	9	- 7.5	- 78.0
5	10a	- 5.7	- 81.3
6	10d	-6.2	-50.4
7	11	-5.7	-89.4
8	camptothecin	-8.1	- 91. 2

In the case of 5-tosyl-hexahydroquinolino[4,3-*b*][1,5]naphthyridine derivatives **8** and 5-tosyl-tetrahydroquinolino[4,3-*b*][1,5]naphthyridin-6(5*H*)-one derivative **9** (Chart 1) two different orientations could be observed (Figures S4 and S5 in the Supporting Material). Compounds **8a,b** (Table 4, entries 1 and 2) are stacked between nucleobases in the rupture zone, where π - π stacking interactions of the phenyl ring of tetracyclic ring system with DA113 are observed. Moreover, a hydrogen bond was established between one oxygen atom of the Ts group and Asn 352 residue, which plays a key role in the modulation of drug binding [22]. The tosyl substituent at position 5 and phenyl substituent at position 7 of the tetracyclic ring system are oriented towards the major groove presenting hydrophobic interactions with Ile 355, Trp 416, Ile 427, Tyr 426 and Ile 424 among other amino acids.

However, another orientation pattern is observed for **8d** (Figure S4 in Supporting Material), since in this case π - π stacking interactions of the phenyl substituent at 7 position with DA113 and

the phenyl ring of Ts group with TGP11 are observed, while the hydrogen bond of one oxygen atom of the Ts group with Asn 352 was maintained. In this case, the substituents of positions 5 and 7 are oriented towards the minor groove of the ADN and the tetracyclic system towards the major groove presenting hydrophobic interactions with several of the residues that limit that area.

Compound **9**, which has the best score value and a similar energy to compounds **8a,b**, is also located between nucleobases in the rupture zone establishing more π - π stacking interactions than the above compounds. On one side, between the aromatic ring of tetrahydroquinolone system and TGP11 and on the other between the pyridine ring, at the other end of the tetracyclic ring system, with DA113. In this way, the tetracyclic system is oriented towards the minor groove near to Arg 364 and the substituents of positions 5 and 7 towards the major groove, where they give hydrophobic interactions with Asn 352 and Pro 431.

For more aromatized compounds **10a-d** and **11** (Figures S6 and S7 in the Supporting Material) the orientation modes are very different. Compound **10a**, which has the worst score value (Table 4, entry 5), although good energy value, directs the tetracyclic system towards the major groove and π - π stacking interactions are observed between the aromatic ring of the Ts group with TGP11 and DA113. In compound **10d** the pyridine ring of the tetracyclic system is oriented towards the minor groove and the benzene ring at the opposite end towards the major groove. This orientation allows π - π stacking interactions to be established between the naphthyridine zone with TGP11 and between the benzene ring at position 7 with DA113. In the case of compound **11**, which has the best energy value, the aromatic ring of tetrahydroquinoline system presents π - π stacking interactions with DA113 and the carbon-nitrogen double bond of Arg 364.

Isosteric substitution of the oxygen atom (O), present in the chromenonaphthyridines **II** (Figure 1), by a tosylamino group, present in the quinolinonaphthyridine derivatives **III** (Figure 1), increases the interaction with the topoisomerase I target. In this sense, the corresponding gscore (gemodel) values result more favourable and may explain the increment of the inhibition of these derivatives **8**, **9**, **10** and **11** towards TopI.

4.4. In silico ADME/T analysis. The synthesized compounds were submitted to *in silico* pharmacokinetic properties prediction by using the graphical interface Maestro [23] and QikProp module of Schrödinger software. The results are included in Table S2 of Supporting Material. Thus, estimated number of hydrogen bonds that would be donated and accepted by the solute to the water molecules in an aqueous solution are in the range of 0.0-2.0 and the 6.5-7.0 respectively. Number of metabolic reactions of compounds **8** and **9** and **15** is high (in the range of 8 to 10), while for more aromatized compounds **10** and **11** is in the range of 2 to 3. All compounds have % Human Oral Absorption of 100%. Prediction of binding to human serum albumin for the compounds are in the range 0.56-1.15 and predicted brain/blood partition coefficient are in the range of -0.44 to 0.043. Number of violations of Lipinsky's rule of five is 0-2. Thus, it was observed that most of the compounds were found to be within the limit of approved drug parameter range.

5. Conclusions

To sum up, the preparation of hybrid 1,5-naphthyridines fused with heterocycles such as quinolines and quinolinones is reported by a regio- and stereospecific intramolecular [4+2]-cycloaddition reaction followed by prototropic tautomerization. Consequent dehydrogenation of hexahydro- and tetrahydro-1,5-naphthyridine core of compounds **8** and **9** gave rise to the corresponding more unsaturated derivatives **10** and **11**, respectively. In a nicking assay is observed that these new

compounds behave as TopI poisons leading to the generation of TopI dependent nicks most probably resulting from accumulated cleavage complexes in plasmid DNA. Moreover, these novel compounds were demonstrated to be potent inhibitors of TopI relaxation activity. Regarding their cytotoxicity, 5-tosyltetrahydroquinolino[4,3-*b*][1,5]naphthyridin-6(5*H*)-one **9** resulted the most cytotoxic compound with IC₅₀ values of 3.25±0.91 μM and 2.08±1.89 μM against the A549 cell line and the SKOV3 cell line, respectively. Moreover, 5-tosylhexahydroquinolino[4,3-*b*][1,5]naphthyridine **8a** and 5-tosyldihydroquinolino[4,3-*b*][1,5]naphthyridine **10a** demonstrated to be cytotoxic with IC₅₀ values of 7.25±0.81 μM and 7.34±0.17 μM against the A549 cell line, respectively, and with IC₅₀ values of 8.08±1.39 μM and 8.65±0.57 μM against the SKOV3 cell line, respectively. None of the compounds had cytotoxic effects against non-malignant pulmonary fibroblasts (MRC-5).

The physicochemical properties of these hybrid compounds have been calculated, pharmacotherapeutic profiles being evaluated. Docking experiments showed us how they interact with the protein active site and the possible mode of binding of these compounds. The interesting biochemical and biological features found for these derivatives provide a promising basis for further development of biologically active naphthyridines.

6. Experimental protocols

6.1 Chemistry

6.1.1. General experimental information

All reagents from commercial suppliers were used without further purification. All solvents were freshly distilled before use from appropriate drying agents. All other reagents were recrystallized

or distilled when necessary. Reactions were performed under a dry nitrogen atmosphere. Analytical TLCs were performed with silica gel 60 F₂₅₄ plates. Visualization was accomplished by UV light. Column chromatography was carried out using silica gel 60 (230-400 mesh ASTM). Melting points were determined with an Electrothermal IA9100 Digital Melting Point Apparatus without correction. NMR spectra were obtained on a Bruker Avance 400 MHz and a Varian VXR 300 MHz spectrometers and recorded at 25 °C. Chemical shifts for ¹H NMR spectra are reported in ppm downfield from TMS, chemical shifts for ¹³C NMR spectra are recorded in ppm relative to internal deuterated chloroform ($\delta = 77.2$ ppm for ¹³C), chemical shifts for ¹⁹F NMR are reported in ppm downfield from fluorotrichloromethane (CFCl₃). Coupling constants (*J*) are reported in Hertz. The terms m, s, d, t, q refer to multiplet, singlet, doublet, triplet, quartet. ¹³C NMR, and ¹⁹F NMR were broadband decoupled from hydrogen nuclei. High resolution mass spectra (HRMS) was measured by EI method with a Agilent LC-Q-TOF-MS 6520 spectrometer.

6.1.2. Compounds Purity Analysis

All synthesized compounds were analyzed by HPLC to determine their purity. The analyses were performed on Agilent 1260 infinity HPLC system (C-18 column, Hypersil, BDS, 5 μ m, 0.4 mm \times 25 mm). All the tested compounds were dissolved in dichloromethane, and 1 μ L of the sample was loaded onto the column. Ethanol and heptane were used as mobile phase, and the flow rate was set at 1.0 mL/min. The maximal absorbance at the range of 190–625 nm was used as the detection wavelength. The purity of all the tested compounds is >95%, which meets the purity requirement by the Journal.

6.1.3. Synthesis of aldehydes 1, 2 and 12

6.1.3.1.1. *General procedure for the synthesis of aldehydes 1 and 2.* To a solution of 2-(aminophenyl)methanol (10 mmol, 1.23 g) in THF (30 mL) was added Et₃N (11 mmol, 1.40 mL) and tosyl chloride (11 mmol, 2.097 g) and was stirred at room temperature for 3 h. The reaction mixture was washed with 0.5 M aqueous solution of HCl (50 mL) and water (50 mL), extracted with dichloromethane (2 x 25 mL), dried over anhydrous MgSO₄ and the solvent was removed under vacuum. The crude was dissolved in THF, and the corresponding halide (12 mmol) in presence of K₂CO₃ (20 mmol, 2.76) was added and the mixture was heated 16 h. The reaction mixture was washed with 2M aqueous solution of NaOH (50 mL) and water (50 mL), extracted

with dichloromethane (2 x 25 mL), dried over anhydrous MgSO₄ and the solvent was removed under vacuum. The reaction crude was dissolved in toluene, MnO₂ (40mmol, 3.47g) was added and was heated to reflux for 24 h. The reaction mixture was filtered on celite and the removal of the solvent under vacuum afforded an oil that was purified by silica gel flash column chromatography using an elution of 05-95% ethyl acetate - hexane to afford products **1** and **2**.

6.1.3.1.2. N-Cinnamyl-N-(2-formylphenyl)-4-methylbenzenesulfonamide (1). The general procedure was followed using 1-(3-bromoprop-1-enyl)benzene (12 mmol, 2.365 g) affording 3.367g (84 %) of a white solid identified as **1**, mp 110-111 °C (ethyl acetate/hexane). ¹H NMR (400 MHz, CDCl₃) δ: 2.46 (s, 3H, CH₃), 4.09 (s, 1H, CH₂), 4.70 (s, 1H, CH₂), 6.09 (dt, 1H, ³J_{HH} = 16.0 Hz, ³J_{HH} = 6.6 Hz, ³J_{HH} = 16 Hz, 1H, =CH₂), 6.34 (d, ³J_{HH} = 16.0 Hz, 1H, H_{arom}), 6.79 (dd, ³J_{HH} = 7.8 Hz, ⁴J_{HH} = 1.2 Hz, 1H, H_{arom}), 7.16-7.53 (m, 11H, H_{arom}), 7.52 (d, ³J_{HH} = 8.0 Hz, 1H, H_{arom}), 10.43 (s, 1H, CHO) ppm. ¹³C {¹H} NMR (75 MHz, CDCl₃) δ: 21.7 (CH₃), 54.3 (CH₂), 122.6 (CH), 126.6 (2CH), 128.0 (2CH), 128.3 (2CH), 128.6 (CH), 128.7 (2CH), 128.8 (CH), 129.8 (2CH), 134.2 (CH), 134.7 (C), 135.4 (CH), 135.9 (C), 136.1 (C), 141.5 (C), 144.3 (C), 190.2 (CHO) ppm. HRMS (EI) calculated for C₂₃H₂₁NO₃S [M]⁺ 391.1242; found 391.1239.

6.1.3.1.3. N-(2-Formylphenyl)-N-tosylcinnamamide (2). The general procedure was followed using 4-phenylbut-3-enoyl chloride (12 mmol, 2.16 g) affording 3.771g (90 %) of a white solid identified as **2**, mp 146-147 °C (ethyl acetate/hexane). ¹H NMR (400 MHz, CDCl₃) δ: 2.38 (s, 3H, CH₃), 5.96 (d, ³J_{HH} = 16.0 Hz, 1H, H_{arom}), 7.13-7.30 (m, 9H, H_{arom}), 7.61-7.66 (m, 3H, H_{arom}), 7.85 (d, ³J_{HH} = 8.5 Hz, 1H, H_{arom}), 8.03 (dd, ³J_{HH} = 7.5 Hz, ³J_{HH} = 2.5 Hz, 1H, H_{arom}), 10.05 (s, 1H, CHO) ppm. ¹³C {¹H} NMR (75 MHz, CDCl₃) δ: 21.9 (CH₃), 117.1 (CH), 128.5 (2CH), 129.0 (2CH), 129.7 (4CH), 130.0 (CH), 130.8 (CH), 131.1 (CH), 131.7 (CH), 133.9 (C), 135.1 (C), 135.2 (CH and C), 137.8 (C), 145.7 (C), 147.2 (CH), 165.3 (CNO), 188.8 (CHO) ppm. HRMS (EI) calculated for C₂₃H₂₁NO₃S [M]⁺ 405.1035; found 405.1094.

6.1.3.1.4. N-(2-Formylphenyl)-4-methyl-N-(3-phenylprop-2-yn-1-yl)benzenesulfonamide (12). To a solution of 2-(aminophenyl)methanol (10 mmol, 1.23 g) in THF (30 mL) was added Et₃N (11 mmol, 1.40 mL) and tosyl chloride (11 mmol, 2.097 g) and was stirred at room temperature for 3 h. The reaction mixture was washed with 0.5 M aqueous solution of HCl (50 mL) and water (50 mL), extracted with dichloromethane (2 x 25 mL), dried over anhydrous MgSO₄ and the solvent was removed under vacuum. The reaction crude was dissolved in THF the corresponding halure

3-bromoprop-1-yne (11 mmol, 1.300 g) was added in presence of K_2CO_3 (20 mmol, 2.76 g) and was heated to reflux for 16 h. The reaction mixture was washed with 2M aqueous solution of NaOH (50 mL) and water (50 mL), extracted with dichloromethane (2 x 25 mL), dried over anhydrous $MgSO_4$, the solvent was removed under vacuum. The reaction crude was dissolved in toluene and MnO_2 (40mmol, 3.47g) was added and the solution was heated to reflux for 24 h. The reaction mixture was filtered on celite and the solvent was removed under vacuum affording an oil that was dissolved in dichloromethane and TEA (10 mmol, 1.391 mL), CuI (0.02 mmol, 0.004g), the corresponding iodide (10 mmol) and $Pd(PPh_2)Cl_2$ (0.01 mmol, 0.004g) were added. The mixture was stirred under nitrogen at room temperature during 8 h, then reaction mixture was filtered on celite and the solvent was removed under vacuum affording an oil that was purified by silica gel flash column chromatography using an elution of 10-90% ethyl acetate - hexane to afford 2.061 g (71 %) of a white solid identified as **12**, mp 113-114 °C (ethyl acetate/hexane). 1H NMR (400 MHz, $CDCl_3$) δ : 2.32 (s, 3H, CH_3), 4.61 (s, 2H, H_{arom}), 6.95-7.50 (m, 12H, H_{arom}), 7.93 (dd, $^3J_{HH} = 7.0$ Hz, $^3J_{HH} = 1.8$ Hz, 1H, H_{arom}), 10.36 (s, 1H, CHO) ppm. ^{13}C $\{^1H\}$ NMR (75 MHz, $CDCl_3$) δ : 21.7 (CH_3), 42.9 (CH_2), 82.4 (C), 86.6 (C), 121.9 (C), 128.3 (2CH), 128.4 (2CH), 128.6 (CH), 128.8 (CH), 128.9 (CH) 129.3 (CH), 129.8 (2CH), 131.6 ("CH), 134.3 (CH), 135.1 (C), 136.1 (C), 141.5 (C), 144.5 (C), 190.3 (CHO) ppm. HRMS (EI) calculated for $C_{23}H_{21}NO_3S$ $[M]^+$ 389.1086; found 389.1068.

6.1.4. Synthesis of aldimines **4**, **5** and **13**

6.1.4.1 General procedure. To a solution of the corresponding aldehyde (1 mmol) in $CHCl_3$ (20 mL) the corresponding 3-aminopyridine (1 mmol) was added in presence of molecular sieves (4Å) and one drop of $BF_3 \cdot Et_2O$. The mixture was refluxed for 16h and checked by 1H NMR and/or ^{19}F NMR spectroscopy. Due to the instability of the aldimines, they were used without purification for the following reactions.

6.1.4.1.1 *N*-Cinnamyl-4-methyl-*N*-(2-(pyridin-3-ylimino)methyl)phenyl)benzenesulfonamide (4a**).** The general procedure was followed using aldehyde **1a** (1 mmol, 0.389 g) and 3-aminopyridine (1 mmol, 0.094 g). 1H NMR (400 MHz, $CDCl_3$) δ : 2.34 (s, 3H, CH_3), 3.99 (dd, $^3J_{HH} = 14.0$ Hz, $^3J_{HH} = 8.5$ Hz, 1H, CH_2), 4.57 (dd, $^3J_{HH} = 14.0$ Hz, $^3J_{HH} = 6.2$ Hz, 1H, CH_2), 6.01 (dt, $^3J_{HH} = 16.0$ Hz, $^3J_{HH} = 7.0$ Hz, 1H, =CH), 6.25 (d, $^3J_{HH} = 16.0$ Hz, 1H, H_{arom}), 6.69 (dd, $^3J_{HH} = 8.0$

Hz, $^3J_{\text{HH}} = 1.2$ Hz, 1H, =CH), 7.08-7.37 (m, 13H, H_{arom}), 7.48 (d, $^3J_{\text{HH}} = 8.0$ Hz, 1H, H_{arom}), 8.21 (dd, $^3J_{\text{HH}} = 8.0$ Hz, $^4J_{\text{HH}} = 1.8$ Hz, 1H, H_{arom}), 8.34 (dd, $^3J_{\text{HH}} = 2.5$ Hz, $^4J_{\text{HH}} = 0.7$ Hz, 1H, H_{arom}), 8.39 (dd, $^3J_{\text{HH}} = 4.8$ Hz, $^4J_{\text{HH}} = 1.5$ Hz, 1H, H_{arom}), 8.73 (s, 1H, C=N) ppm.

6.1.4.1.2 *N*-(2-(((4-Bromopyridin-3-yl)imino)methyl)phenyl)-*N*-cinnamyl-4-methylbenzene sulfonamide (**4d**). The general procedure was followed using aldehyde **1** (1 mmol, 0.391 g) and 4-bromopyridin-3-amine (1 mmol, 0.171 g). ^1H NMR (400 MHz, CDCl_3) δ : 2.43 (s, 3H, CH_3), 4.04 (dd, $^3J_{\text{HH}} = 14.0$ Hz, $^3J_{\text{HH}} = 8.2$ Hz, 1H, CH_2), 4.70 (dd, $^3J_{\text{HH}} = 14.0$ Hz, $^3J_{\text{HH}} = 6.0$ Hz, 1H, CH_2), 6.88 (dt, $^3J_{\text{HH}} = 16.0$ Hz, $^3J_{\text{HH}} = 7.2$ Hz, 1H, =CH), 6.36 (d, $^3J_{\text{HH}} = 16.0$ Hz, 1H, H_{arom}), 6.71 (d, $^3J_{\text{HH}} = 8.0$ Hz, 1H, =CH), 7.18-7.55 (m, 13H, H_{arom}), 8.20 (dd, $^3J_{\text{HH}} = 4.4$ Hz, $^4J_{\text{HH}} = 1.8$ Hz, 1H, H_{arom}), 8.40 (d, $^3J_{\text{HH}} = 7.5$ Hz, 1H, H_{arom}), 8.79 (s, 1H, C=N) ppm.

6.1.4.1.3 *N*-(2-((Pyridin-3-ylimino)methyl)phenyl)-*N*-tosylcinnamamide (**5**). The general procedure was followed using using aldehyde **2** (1 mmol, 0.405 g) and 3-aminopyridine (1 mmol, 0.096 g). ^1H NMR (400 MHz, CDCl_3) δ : 2.29 (s, 3H, CH_3), 5.96 (d, $^3J_{\text{HH}} = 16.0$ Hz, 1H, H_{arom}), 7.12-7.70 (m, 16H, H_{arom}), 7.88 (d, $^3J_{\text{HH}} = 8.4$ Hz, 1H, H_{arom}), 8.46 (s, 1H, C=N) ppm.

6.1.4.1.4 *4-Methyl-N*-(3-phenylprop-2-yn-1-yl)-*N*-(2-((pyridin-3-ylimino)methyl)phenyl) benzenesulfonamide (**13**). The general procedure was followed using aldehyde **12** (1 mmol, 0.389 g) and 3-aminopyridine (1 mmol, 0.096 g). ^1H NMR (400 MHz, CDCl_3) δ : 2.39(s, 3H, CH_3), 4.60-4.79 (m, 1H, H_{arom}), 7.00-7.63 (m, 16H, H_{arom}), 8.36 (dd, $^3J_{\text{HH}} = 7.8$ Hz, $^3J_{\text{HH}} = 1.6$ Hz, 1H, H_{arom}), 8.89 (s, 1H, C=N) ppm.

6.1.5. Synthesis of hexahydroquinolino-6H-[4,3-b][1,5]naphthyridines **8 and dihydroquinolino-6H-[4,3-b][1,5]naphthyridin-6(5H)-ones **9****

6.1.5.1 General procedure. To a solution of the corresponding aldimine (1 mmol) generated *in situ* in CHCl_3 (20 mL), $\text{BF}_3 \cdot \text{Et}_2\text{O}$ was added and the reaction was refluxed for 16 h. The reaction mixture was washed with 2M aqueous solution of NaOH (50 mL) and water (50 mL), extracted with dichloromethane (2 x 25 mL), and dried over anhydrous MgSO_4 . The solvent was removed under vacuum affording an oil that was purified by silica gel flash column chromatography using an elution of 20-80% ethyl acetate - hexane to afford products **8** or **10**.

6.1.5.1.1 7-Phenyl-5-tosyl-5,6,6a,7,12,12a-hexahydroquinolino[4,3-b][1,5]naphthyridine (8a).

The general procedure was followed using aldimine **4a** and $\text{BF}_3 \cdot \text{Et}_2\text{O}$ (2 mmol, 0.25 mL) affording 0.284 (88 %) of a white solid identified as **8a**, mp 190-191 °C (ethyl acetate/hexane). ^1H NMR (400 MHz, CDCl_3) δ : 1.90 (dddd, $^3J_{\text{HH}} = 11.3$ Hz, $^3J_{\text{HH}} = 11.3$ Hz, $^3J_{\text{HH}} = 10.7$ Hz, $^3J_{\text{HH}} = 4.2$ Hz, 1H, CH), 2.34 (s, 3H, CH_3), 3.36 (dd, $^3J_{\text{HH}} = 14.0$ Hz, $^3J_{\text{HH}} = 11.3$ Hz, 1H, CH_2), 3.85 (d, $^3J_{\text{HH}} = 11.0$ Hz, 1H, CH_2), 3.98 (d, $^3J_{\text{HH}} = 10.7$ Hz, 1H, CH), 4.05 (dd, $^3J_{\text{HH}} = 14.0$ Hz, $^3J_{\text{HH}} = 4.2$ Hz, 1H, H_{arom}), 4.22 (s, 1H, NH), 6.94-7.38 (m, 14H, H_{arom}), 7.95 (dd, $^3J_{\text{HH}} = 4.2$ Hz, $^4J_{\text{HH}} = 1.8$ Hz, 1H, H_{arom}), 7.99 (dd, $^3J_{\text{HH}} = 8.6$ Hz, $^4J_{\text{HH}} = 2.0$ Hz, 1H, H_{arom}) ppm. ^{13}C $\{^1\text{H}\}$ NMR (75 MHz, CDCl_3) δ : 21.7 (CH_3), 41.5 (CH), 48.6 (CH_2), 51.6 (CH), 53.3 (CH), 122.2 (CH), 122.8 (CH), 124.5 (CH), 125.1 (CH), 125.4 (CH), 127.2 (3 CH), 128.2 (C), 128.9 (2 CH), 129.2 (2 CH), 129.6 (C), 129.8 (2 CH), 136.0 (C), 136.3 (C), 140.7 (CH), 140.8 (C), 142.0 (C), 143.8 (C), 145.1 (C) ppm. HRMS (EI) calculated for $\text{C}_{28}\text{H}_{25}\text{N}_3\text{O}_2\text{S}$ $[\text{M}]^+$ 467.1667; found 467.1666. Purity 96.00 % (EtOH/Heptane = 10/90, $R_t = 7.30$ min).

6.1.5.1.2 9-Methoxy-7-phenyl-5-tosyl-5,6,6a,7,12,12a-hexahydroquinolino[1,2-b][1,5]naphthyridine (8b).

The general procedure was followed using aldimine **4b** and $\text{BF}_3 \cdot \text{Et}_2\text{O}$ (2 mmol, 0.25 mL) affording 0.422 g (85 %) of a white solid identified as **8b**, mp 235-236 °C (ethyl acetate/hexane). ^1H NMR (400 MHz, CDCl_3) δ : 1.75 (dddd, $^3J_{\text{HH}} = 11.0$ Hz, $^3J_{\text{HH}} = 11.0$ Hz, $^3J_{\text{HH}} = 11.0$ Hz, $^3J_{\text{HH}} = 4.0$ Hz, 1H, CH), 2.25 (s, 3H, CH_3), 3.26 (dd, $^3J_{\text{HH}} = 14.0$ Hz, $^3J_{\text{HH}} = 11.0$ Hz, 1H, CH_2), 3.38 (s, 3H, OCH_3), 3.65 (d, $^3J_{\text{HH}} = 11.0$ Hz, 1H, CH_2), 3.85 (d, $^3J_{\text{HH}} = 11.0$ Hz, 1H, CH), 4.08 (dd, $^3J_{\text{HH}} = 14.0$ Hz, $^3J_{\text{HH}} = 4.0$ Hz, 1H, H_{arom}), 6.37 (d, $^3J_{\text{HH}} = 7.8$ Hz, 1H, CH_{arom}), 6.86-7.26 (m, 14H, H_{arom}), 7.90 (d, $^3J_{\text{HH}} = 9.10$ Hz, 1H, CH_{arom}) ppm. ^{13}C $\{^1\text{H}\}$ NMR (75 MHz, CDCl_3) δ : 21.7 (CH_3), 40.9 (CH), 48.7 (CH_2), 51.2 (CH), 53.1 (OCH_3), 54.1 (CH), 109.4 (CH), 124.8 (CH), 125.1 (CH), 125.4 (CH), 126.8 (CH), 127.2 (2 CH), 128.2 (CH), 128.3 (2 CH), 129.1 (2 CH), 129.4 (2 CH), 129.8 (CH and C), 134.5 (C), 136.0 (C), 136.4 (C), 141.4 (C), 142.0 (C), 143.7 (C), 157.3 (C) ppm. HRMS (EI) calculated for $\text{C}_{29}\text{H}_{27}\text{N}_3\text{O}_3\text{S}$ $[\text{M}]^+$ 497.1773; found 497.1769. Purity 98.60 % (EtOH/Heptane = 10/90, $R_t = 6.90$ min).

6.1.5.1.3 9-Bromo-7-phenyl-5-tosyl-5,6,6a,7,12,12a-hexahydroquinolino[4,3-b][1,5]naphthyridine (8c).

The general procedure was followed using aldimine **4c** and $\text{BF}_3 \cdot \text{Et}_2\text{O}$ (2 mmol, 0.25 mL) affording 0.465 g (85 %) of a white solid identified as **8c**, mp 238-239 °C (ethyl acetate/hexane). ^1H NMR (400 MHz, CDCl_3) δ : 1.85 (dddd, $^3J_{\text{HH}} = 11.0$ Hz, $^3J_{\text{HH}} = 11.0$ Hz, $^3J_{\text{HH}}$

= 10.0 Hz, $^3J_{\text{HH}} = 4.7$ Hz, 1H, CH), 2.37 (s, 3H, CH₃), 3.35 (dd, $^3J_{\text{HH}} = 14.0$ Hz, $^3J_{\text{HH}} = 11.0$ Hz, 1H, CH₂), 3.81 (d, $^3J_{\text{HH}} = 11.0$ Hz, 1H, CH₂), 3.98 (d, $^3J_{\text{HH}} = 10.0$ Hz, 1H, CH), 4.10 (dd, $^3J_{\text{HH}} = 14.0$ Hz, $^3J_{\text{HH}} = 4.7$ Hz, 1H, H_{arom}), 4.25 (s, 1H, NH), 6.86 (d, $^3J_{\text{HH}} = 9.0$ Hz, 1H, CH_{arom}), 6.94-7.39 (m, 14H, H_{arom}), 8.00 (d, $^3J_{\text{HH}} = 8.4$ Hz, 1H, CH_{arom}) ppm. ¹³C {¹H} NMR (75 MHz, CDCl₃) δ: 21.7 (CH₃), 41.2 (CH), 48.4 (CH₂), 51.2 (CH), 53.4 (CH), 124.5 (CH), 125.1 (CH), 125.4 (CH), 125.9 (CH), 126.5 (CH), 127.2 (3 CH), 128.4 (CH), 128.7 (2 CH), 129.0 (C), 129.3 (2 CH), 129.8 (2 CH), 129.9 (C), 135.9 (C), 136.3 (C), 140.3 (C), 141.2 (C), 143.8 (C), 145.7 (C) ppm. HRMS (EI) calculated for C₂₈H₂₄BrN₃O₂S [M]⁺ 545.0773; found 545.0742. Purity 96.60 % (EtOH/Heptane = 10/90, Rt = 6.80 min).

6.1.5.1.4 11-Bromo-7-phenyl-5-tosyl-5,6,6a,7,12,12a-hexahydroquinolino[4,3-b][1,5]naphthyridine (8d). The general procedure was followed using aldimine **4b** and BF₃·Et₂O (2 mmol, 0.25 mL) affording 0.386 g (70 %) of a white solid identified as **8d**, mp 201-202 °C (ethyl acetate/hexane). ¹H NMR (400 MHz, CDCl₃) δ: 1.84 (dddd, $^3J_{\text{HH}} = 11.2$ Hz, $^3J_{\text{HH}} = 11.5$ Hz, $^3J_{\text{HH}} = 10.5$ Hz, $^3J_{\text{HH}} = 5.0$ Hz, 1H, CH), 2.29 (s, 3H, CH₃), 3.23 (dd, $^3J_{\text{HH}} = 13.8$ Hz, $^3J_{\text{HH}} = 11.2$ Hz, 1H, CH₂), 3.60 (d, $^3J_{\text{HH}} = 11.2$ Hz, 1H, CH₂), 3.84 (dd, $^3J_{\text{HH}} = 13.5$ Hz, $^3J_{\text{HH}} = 5.0$ Hz, 1H, H_{arom}), 3.83 (d, $^3J_{\text{HH}} = 10.5$ Hz, 1H, CH), 4.83 (s, 1H, NH), 6.33 (d, $^3J_{\text{HH}} = 4.8$ Hz, 1H, CH_{arom}), 6.82-7.47 (m, 14H, H_{arom}), 7.85-7.89 (m, 1H, CH_{arom}) ppm. ¹³C {¹H} NMR (75 MHz, CDCl₃) δ: 21.7 (CH₃), 40.0 (CH), 48.6 (CH₂), 48.7 (CH), 53.2 (CH), 123.9 (CH), 124.1 (CH), 125.2 (CH), 125.7 (CH), 127.1 (2 CH), 128.1 (CH), 128.4 (CH), 128.5 (C), 128.9 (C), 129.3 (2 CH), 129.6 (C), 129.9 (CH), 129.9 (CH), 133.8 (C), 135.8 (C), 136.0 (C), 137.8 (CH), 138.4 (CH), 138.8 (C), 139.9 (C), 144.1 (C) ppm. HRMS (EI) calculated for C₂₈H₂₄N₃BrO₂S [M]⁺ 545.0773; found 545.0742. Purity 95.10 % (EtOH/Heptane = 10/90, Rt = 7.20 min).

6.1.5.1.5 7-Phenyl-5-tosyl-6a,7,12,12a-tetrahydroquinolino[4,3-b][1,5]naphthyridin-6(5H)-one (9). The general procedure was followed using aldimine **5** and BF₃·Et₂O (2 mmol, 0.25 mL) affording 0.456 g (95 %) of a white solid identified as **9**, mp 270-271 °C (ethyl acetate/hexane). ¹H NMR (400 MHz, CDCl₃) δ: 2.39 (s, 3H, CH₃), 3.06 (dd, $^3J_{\text{HH}} = 12.0$ Hz, $^3J_{\text{HH}} = 9.0$ Hz, 1H, CH₂), 4.32 (d, $^3J_{\text{HH}} = 9.0$ Hz, 1H, CH₂), 4.36 (d, $^3J_{\text{HH}} = 12.0$ Hz, 1H, CH), 6.71 (s, 1H, NH), 6.97-7.89 (m, 16H, H_{arom}) ppm. ¹³C {¹H} NMR (75 MHz, CDCl₃) δ: 21.1 (CH₃), 45.4 (CH), 48.7 (CH), 51.75 (CH), 121.9 (CH), 122.2 (CH), 123.6 (CH), 123.9 (CH), 125.7 (CH), 126.4 (CH), 127.4 (CH), 127.9 (2 CH), 128.0 (2 CH), 129.1 (2 CH), 129.8 (2 CH), 132.0 (C), 132.8 (C), 136.1 (C),

139.4 (C), 140.0 (CH), 144.6 (C), 145.1 (C), 145.3 (C), 170.5 (CO) ppm. HRMS (EI) calculated for $C_{28}H_{33}N_3O_3S$ $[M]^+$ 467.1667; found 481.1461. Purity 98.40 % (EtOH/Heptane = 10/90, R_t = 8.05 min).

6.1.6. Synthesis of quinolino[4,3-*b*][1,5]naphthyridines **10** and quinolino[4,3-*b*][1,5]naphthyridin-6(5*H*)-one **11**

6.1.6.1 General procedure A. To a solution of the corresponding naphthyridine derivative (1 mmol) in toluene (20 mL) MnO_2 (4 mmol, 0.347 g) was added and the reaction was refluxed for 24 h. The reaction mixture was filtered on celite, washed with dichloromethane (2 x 10 mL), and dried over anhydrous $MgSO_4$. The solvent was removed under vacuum affording an oil that was purified by silica gel flash column chromatography using an elution of 20-80% ethyl acetate - hexane to afford products **10** and **11**.

General procedure B. To a solution of the corresponding aldehyde **12** (1 mmol, 0.389 g) in $CHCl_3$ (20 mL), the corresponding 3-aminopyridine (1 mmol) was added in presence of molecular sieves (4Å). Then, $BF_3 \cdot Et_2O$ was added and the reaction was refluxed for 12 h. The reaction mixture was washed with 2M aqueous solution of NaOH (50 mL) and water (50 mL), extracted with dichloromethane (2 x 25 mL), and dried over anhydrous $MgSO_4$. The solvent was removed under vacuum affording an oil that was purified by silica gel flash column chromatography using an elution of 20-80% ethyl acetate - hexane to afford products **10**.

6.1.6.1.1 7-Phenyl-5-tosyl-5,6-dihydroquinolino[4,3-*b*][1,5]naphthyridine (10a). The general procedure A was followed using naphthyridine **8a** 0.463g (99%) of a white solid identified as **10a**, mp 193-194 °C (ethyl acetate/hexane). When the procedure B was followed using aldimine **13a** and $BF_3 \cdot Et_2O$ (2 mmol, 0.25 mL), 0.393 g (85 %) of compound **10a** were obtained. 1H NMR (400 MHz, $CDCl_3$) δ : 1.90 (s, 3H, CH_3), 4.93 (s, 2H, CH_2), 6.66 (d, $^3J_{HH} = 7.8$ Hz, 1H, CH), 6.97 (d, $^3J_{HH} = 8.5$ Hz, 1H, CH), 7.36-7.65 (m, 8H, CH), 7.81 (dd, $^3J_{HH} = 14.0$ Hz, $^3J_{HH} = 8.0$ Hz, 1H, CH), 7.81 (dd, $^3J_{HH} = 8.2$ Hz, $^4J_{HH} = 1.6$ Hz, 1H, CH), 8.30 (dd, $^3J_{HH} = 8.2$ Hz, $^4J_{HH} = 2.0$ Hz, 1H, CH), 8.30 (dd, $^3J_{HH} = 4.2$ Hz, $^4J_{HH} = 1.8$ Hz, 1H, CH) ppm. ^{13}C $\{^1H\}$ NMR (75 MHz, $CDCl_3$) δ : 21.1 (CH_3), 48.1 (CH_2), 124.0 (CH), 126.4 (CH), 126.5 (C), 121.1 (2 CH), 128.0 (2 CH), 128.7 (2 CH), 128.8 (2 CH), 129.2 (CH), 130.2 (2 CH), 130.8 (C), 131.1 (CH), 133.7 (C), 134.5 (C), 137.0 (CH), 138.4 (C), 141.6 (C), 143.2 (C), 143.7 (C), 145.2 (C), 150.3 (C), 150.8 (CH) ppm. HRMS (EI)

calculated for C₂₈H₂₁N₃O₂S [M]⁺ 463.1354; found 463.1363. Purity 97.00 % (EtOH/Heptane = 10/90, Rt = 6.35 min).

6.1.6.1.2 9-Methoxy-7-phenyl-5-tosyl-5,6-dihydroquinolino[4,3-b][1,5]naphthyridine (10b).

The general procedure A was followed using naphthyridine **9b** 0.493 g (99%) of a white solid identified as **10a**, mp 218-219 °C (ethyl acetate/hexane). When the procedure B was followed using aldimine **13b** and BF₃·Et₂O (2 mmol, 0.25 mL), 0.468 g (95 %) of compound **10b** were obtained. T. ¹H NMR (400 MHz, CDCl₃) δ: 1.95 (s, 3H, CH₃), 3.82 (s, 3H, OCH₃), 4.96 (s, 2H, CH₂), 6.68 (d, ³J_{HH} = 8.0 Hz, 2H, CH), 6.95 (d, ³J_{HH} = 8.0 Hz, 2H, CH), 7.04 (d, ³J_{HH} = 9.0 Hz, 1H, CH), 7.38-7.80 (m, 7H, CH), 7.79 (dd, ³J_{HH} = 8.0 Hz, ⁴J_{HH} = 1.2 Hz, 1H, CH), 8.10 (d, ³J_{HH} = 8.8 Hz, 1H, CH), 8.30 (dd, ³J_{HH} = 7.5 Hz, ⁴J_{HH} = 2.0 Hz, 1H, CH) ppm. ¹³C {¹H} NMR (75 MHz, CDCl₃) δ: 21.2 (CH₃), 48.1 (CH₂), 53.7 (CH₃), 116.0 (CH), 125.9 (C), 125.9 (CH), 127.1 (2 CH), 127.9 (2 CH), 128.2 (2 CH), 128.7 (2 CH and C), 130.4 (CH), 130.5 (2 CH), 131.2 (C), 133.9 (CH), 134.6 (C), 137.7 (C), 139.2 (C), 139.9 (CH), 141.1(C), 143.2 (C), 143.6 (C), 147.4 (C), 161.8 (C) ppm. HRMS (EI) calculated for C₂₉H₂₃N₃O₂S [M]⁺ 493.1460; found 493.1442. Purity 95.31 % (EtOH/Heptane = 10/90, Rt = 6.15 min).

6.1.6.1.3 9-Bromo-7-phenyl-5-tosyl-5,6-dihydroquinolino[4,3-b][1,5]naphthyridine (10c).

The general procedure A was followed using naphthyridine **9c** 0.541 g (99%) of a white solid identified as **10c**, mp 235-236 °C (ethyl acetate/hexane). When the procedure B was followed using aldimine **13c** and BF₃·Et₂O (2 mmol, 0.25 mL), 0.476 g (88 %) of compound **10c** were obtained. ¹H NMR (400 MHz, CDCl₃) δ: 1.94 (s, 3H, CH₃), 4.95 (s, 2H, CH₂), 6.69 (d, ³J_{HH} = 8.0 Hz, 2H, CH), 6.94 (d, ³J_{HH} = 9.0 Hz, 2H, CH), 7.35-7.66 (m, 8H, CH), 7.80 (dd, ³J_{HH} = 8.0 Hz, ⁴J_{HH} = 2.0 Hz, 1H, CH), 8.09 (d, ³J_{HH} = 8.8 Hz, 1H, CH), 8.33 (dd, ³J_{HH} = 8.0 Hz, ⁴J_{HH} = 2.0 Hz, 1H, CH) ppm. ¹³C {¹H} NMR (75 MHz, CDCl₃) δ: 21.2 (CH₃), 48.0 (CH₂), 126.4 (CH), 127.1 (2 CH), 128.0 (2 CH), 128.2 (2 CH), 128.5 (CH), 128.9 (2 CH), 129.2 (CH), 129.3 (CH), 130.5 (2 CH), 131.4 (CH), 132.0 (CH), 132.7 (C), 134.2 (C), 138.3 (C), 139.3 (CH), 141.6 (C), 141.8 (C), 142.3 (C), 143.7 (C), 144.5 (C), 150.6 (C) ppm. HRMS (EI) calculated for C₂₈H₂₀BrN₃O₂S [M]⁺ 541.0460; found 541.0435. Purity 95.02 % (EtOH/Heptane = 10/90, Rt = 6.55 min).

6.1.6.1.4 11-Bromo-7-phenyl-5-tosyl-5,6-dihydroquinolino[4,3-b][1,5]naphthyridine (10d).

The general procedure A was followed using naphthyridine **9d** 0.541 g (99%) of a white solid identified

as **10d**, mp 205-206 °C (ethyl acetate/hexane). When the procedure B was followed using aldimine **13d** and BF₃·Et₂O (2 mmol, 0.25 mL), 0.362 g (67 %) of compound **10d** were obtained. ¹H NMR (400 MHz, CDCl₃) δ: 2.01 (s, 3H, CH₃), 4.86 (s, 2H, CH₂), 6.70 (d, ³J_{HH} = 8.0 Hz, 1H, CH), 6.93 (d, ³J_{HH} = 9.0 Hz, 1H, CH), 7.25-7.28 (m, 3H, CH), 7.52-7.68 (m, 5H, CH), 7.78 (d, ³J_{HH} = 8.8 Hz, 1H, CH), 8.18 (d, ³J_{HH} = 8.0 Hz, 1H, CH) ppm. ¹³C {¹H} NMR (75 MHz, CDCl₃) δ: 21.3 (CH₃), 47.8 (CH₂), 118.7 (CH), 127.1 (2 CH), 127.2 (CH), 127.7 (C), 127.8 (CH), 128.3 (CH), 128.9 (2 CH), 129.2 (2 CH), 129.5 (2 CH), 129.8 (CH), 130.5 (C), 131.3 (C), 131.8 (CH), 133.0 (C), 133.9 (C), 138.4 (C), 140.8 (C), 142.6 (CH), 144.1 (C), 144.4 (C), 148.3 (C), 151.6 (C) ppm. HRMS (EI) calculated for C₂₈H₂₀BrN₃O₂S [M]⁺ 541.0460; found 541.0435. Purity 96.45 % (EtOH/Heptane = 10/90, Rt = 6.70 min).

6.1.6.1.5 7-Phenyl-5-tosylquinolino[4,3-b][1,5]naphthyridin-6(5H)-one (11). The general procedure A was followed using **9** 0.477 g (99%) of a white solid identified as **11**, mp >300 °C (ethyl acetate/hexane). ¹H NMR (400 MHz, DMSO-d₆) δ: 2.46 6.95 (d, ³J_{HH} = 9.3 Hz, 2H, CH), 7.26-7.73 (m, 11H, CH), 8.61 (dd, ³J_{HH} = 8.7 Hz, ⁴J_{HH} = 1.6 Hz, 1H, CH), 8.90 (dd, ³J_{HH} = 8.7 Hz, ⁴J_{HH} = 1.6 Hz, 1H, CH), 8.99 (dd, ³J_{HH} = 4.0 Hz, ⁴J_{HH} = 2.0 Hz, 1H, CH) ppm. ¹³C {¹H} NMR (75 MHz, DMSO-d₆) δ: 21.2 (CH₃), 101.6 (2 CH), 113.7 (2 CH), 119.5 (C), 121.9 (C), 125.1 (C), 126.3 (C), 127.0 (C), 128.3 (CH), 128.7 (CH), 129.2 (2 CH), 129.9 (CH), 131.3 (CH), 135.3 (CH), 135.5 (CH), 135.7 (CH), 136.8 (CH), 137.1 (C), 141.0 (C), 145.4 (C), 150.8 (2 CH), 152.2 (C), 152.7 (C), 161.1 (CO) ppm. HRMS (EI) calculated for C₂₈H₁₉N₃O₃S [M]⁺ 477.1147; found 477.1138. Purity 98.00 % (EtOH/Heptane = 10/90, Rt = 7.20 min).

6.1.7. Synthesis of hexahydroquinolino[4,3-b][1,5]naphthyridines 15 derivatives

6.1.7.1 General procedure A. To a solution of the corresponding naphthyridine **8** (1 mmol) in MeOH (10 mL) Mg (2 mmol, 0.049) was added and the reaction was sonicated for 8 h. The reaction mixture was washed with 6M aqueous solution of HCl until pH 7 and water (50 mL), extracted with dichloromethane (2 x 25 mL), and dried over anhydrous MgSO₄. The solvent was removed under vacuum affording an oil that was purified by silica gel flash column chromatography using an elution of 30-70% ethyl acetate - hexane to afford products **15**.

6.1.7.1.1 7-Phenyl-5,6,6a,7,12,12a-hexahydroquinolino[4,3-b][1,5]naphthyridine (15a). The general procedure was followed using **8a** affording 0.463 g (99%) of a white solid identified as

15a, mp 201-202 °C (ethyl acetate/hexane). ¹H NMR (400 MHz, CDCl₃) δ: 3.10 (d, ³J_{HH} = 1.9 Hz, 1H, CH), 3.03 (s, 1H, CH₂), 3.83 (s, 1H, NH), 3.86 (d, ³J_{HH} = 12.0 Hz, 1H, CH), 4.33 (s, 1H, NH), 4.37 (d, ³J_{HH} = 10.5 Hz, 1H, CH), 6.40 (dd, ³J_{HH} = 8.0 Hz, ⁴J_{HH} = 1.0 Hz, 1H, CH), 6.27-2.35 (m, 1H, CH), 6.66 (dt, ³J_{HH} = 8.0 Hz, ⁴J_{HH} = 1.0 Hz, 1H, CH), 6.86-7.03 (m, 5H, H_{arom}), 7.12-7.25 (m, 4H, H_{arom}), 7.86 (dd, ³J_{HH} = 4.6 Hz, ⁴J_{HH} = 1.5 Hz, 1H, CH), ppm. ¹³C {¹H} NMR (75 MHz, CDCl₃) δ: 42.1 (CH), 44.2 (CH₂), 51.6 (CH), 53.1 (CH), 114.6 (CH), 117.4 (CH), 120.4 (C), 122.2 (CH), 122.7 (CH), 124.7 (CH), 126.8 (CH), 128.4 (CH), 128.7 (2 CH), 129.2 (2 CH), 140.2 (CH), 141.2 (C), 143.1 (C), 139.3 (CH), 144.1 (C), 145.6 (C) ppm. HRMS (EI) calculated for C₂₁H₁₉N₃ [M]⁺ 467.1167; 467.1115. Purity 98.02 % (EtOH/Heptane = 10/90, Rt = 8.00 min).

6.1.7.1.2 9-Bromo-7-phenyl-5,6,6a,7,12,12a-hexahydroquinolino[4,3-b][1,5]naphthyridine (15b). The general procedure was followed using **8d** affording 0.226 g (58%) of a white solid identified as **15b**, mp 211-212 °C (ethyl acetate/hexane). ¹H NMR (400 MHz, CDCl₃) δ: 2.22-2.31 (m, 2H, CH and NH), 3.01-3.04 (m, 2H, CH₂), 3.81 (d, ³J_{HH} = 12 Hz, 1H, CH), 4.28 (s, 1H, NH), 4.35 (d, ³J_{HH} = 11 Hz, 1H, CH), 6.41 (d, ³J_{HH} = 8.0 Hz, 1H, CH), 6.66 (t, ³J_{HH} = 7.6 Hz, 1H, CH), 6.81 (d, ³J_{HH} = 8.8 Hz, 1H, CH), 6.97-7.08 (m, 4H, H_{arom}), 7.10-7.27 (m, 7H, H_{arom}) ppm. ¹³C {¹H} NMR (75 MHz, CDCl₃) δ: 41.9 (CH), 44.1 (CH₂), 51.3 (CH), 53.1 (CH), 114.7 (CH), 117.5 (CH), 120.0 (C), 124.6 (CH), 125.7 (CH), 126.4 (2 CH), 126.8 (CH), 128.5 (2 CH), 129.3 (2 CH), 129.4 (C), 140.7 (C), 142.3 (C), 144.1 (C), 146.4 (C) ppm. HRMS (EI) calculated for C₂₁H₁₈BrN₃ [M]⁺ 391.0684; 391.0684. Purity 95.30 % (EtOH/Heptane = 10/90, Rt = 7.90 min).

6.2 Biology

6.2.1. Materials

Reagents and solvents were used as purchased without further purification. Camptothecin was purchased from Sigma-Aldrich. All stock solutions of the investigated compounds were prepared by dissolving the powdered materials in appropriate amounts of DMSO. The final concentration of DMSO never exceeded 5% (v/v) in reactions. Under these conditions, DMSO was also used in the

controls and was not seen to affect TopI activity. The stock solution was stored at 5°C until it was used.

6.2.2. Expression and purification of Human Topoisomerase IB.

The yeast *Saccharomyces cerevisiae* TopI null strain RS190, which was used for expression of recombinant human TopI was a kind gift from R. Sternglanz (State University of New York, Stony Brook, NY). Plasmid pHT143, for expression of recombinant TopI under the control of an inducible GAL promoter was described [24]. The plasmids pHT143 were transformed into the yeast *S.cerevisiae* strain RS190. The proteins were expressed and purified by affinity chromatography essentially as described [25]. The protein concentrations were estimated from Coomassie blue-stained SDS/polyacrylamide gels by comparison to serial dilutions of bovine serum albumin (BSA).

6.2.3. DNA relaxation assays.

TopI activity was assayed using a DNA relaxation assay by incubating 110 ng/μL of TopI with 0.5 μg of negatively supercoiled pUC18 in 20 μl of reaction buffer (20 mM Tris-HCl, 0.1 mM Na₂EDTA, 10 mM MgCl₂, 50 μg/ml acetylated BSA and 150 mM KCl, pH 7.5). The effect of the synthesized tetracyclic **8**, **9**, **10**, **11** and **15** derivatives on topoisomerase activity was measured by adding the compounds, at different time points as indicated in the text. The reactions were performed at 37°C, stopped by the addition of 0.5% SDS after indicated time intervals. The samples were protease digested, electrophoresed in a horizontal 1% agarose gel in 1xTBE (50 mM Tris, 45 mM boric acid, 1 mM EDTA) at 26V during 20 hours. The gel was stained with gel red (BIOTIUM, 5 μg/ml), destained with water and photographed under UV illumination.

Since all drugs were dissolved in dimethyl sulfoxide (DMSO), a positive control sample containing the same DMSO concentration as the samples incubated with the drugs was included in all experiments. As a control for drug inhibition the well know TopI specific drug camptothecin was included.

6.2.4. DNA nicking assays.

TopI activity was assayed using a DNA relaxation assay by incubating 330 ng/ μ L of TopI with 0.5 μ g of negatively supercoiled pUC18 in 20 μ l of reaction buffer (20 mM Tris-HCl, 0.1 mM Na₂EDTA, 10 mM MgCl₂, 50 μ g/ml acetylated BSA and 150 mM KCl, pH 7.5). The effect of the synthesized tetracyclic **8**, **9**, **10**, **11** and **15** derivatives on topoisomerase activity was measured by adding the compounds, at different time points as indicated in the text. The reactions were performed at 37°C, stopped by the addition of 0.5% SDS after indicated time intervals. The samples were protease digested, electrophoresed in a horizontal 1% agarose gel in 1xTBE (50 mM Tris, 45 mM boric acid, 1 mM EDTA) containing 0.5 μ g/ml EtBr at 26V during 20 hours.

Since all drugs were dissolved in dimethyl sulfoxide (DMSO), a positive control sample containing the same DMSO concentration as the samples incubated with the drugs was included in all experiments. As a control the well known TopI poison drug camptothecin was included.

The cleavage-ligation equilibrium was investigated by incubating 200 nM of Cy3-labelled DNA substrate (5'-Cy3-ATTTGACCTCGAGAATTATACGAAGTTATTAC-3'/5'-GTAATAACTTCGTATAATTCTCGAGGTCAAAT-3') with 44 nM of TopI, and DMSO, CPT or either compounds **8a**, **10a** or **9** as indicated in figure 4 in a reaction buffer containing 5 mM of MgCl₂, 5 mM of CaCl₂, 10 mM of Tris-HCl pH 7.8 and 100 mM of NaCl for 10 minutes at 37°C.

The reactions were stopped by the addition of SDS to a final concentration of 0.2%, EtOH precipitated and trypsinized following standard protocols as described in (<https://doi.org/10.1039/C6NR06848K>). The reaction products were analyzed in a 20% denaturing polyacrylamide gel (<https://doi.org/10.1039/C6NR06848K>) and the product visualized by a Typhoon Scanner FLA 9500.

6.2.5. Cytotoxicity assays.

Cells were cultured according to the supplier's instructions. Cells were seeded in 96-well plates at a density of $2-2.5 \times 10^3$ cells per well and incubated overnight in 0.1 mL of media supplied with 10% Fetal Bovine Serum (Lonza) in 5% CO₂ incubator at 37 °C. On day 2, drugs were added and samples were incubated for 48 hours. After treatment, 10 µL of cell counting kit-8 was added into each well for additional 2 hours incubation at 37 °C. The absorbance of each well was determined by an Automatic Elisa Reader System at 450 nm wavelength. Camptothecin was purchased from Sigma-Aldrich and used as positive control.

6.3 Computational methodology

6.3.1. Molecular modeling

All calculations included in this paper were carried out with Gaussian 16 program [26] within the density functional theory (DFT) framework [17] using the B3LYP,[18] along with the standard 6-31G** basis set. All minima were fully characterized by harmonic frequency analysis [27]. The solvent effect in DFT calculations was evaluated by means of the Polarizable Continuum Model (PCM) [28] using water as solvent. The pKa values were studied to determine the dominant species (ionization states) at physiological pH (pH = 7.4) using Epik [29] and these were the species used

in each case. After a conformational search with MacroModel [30] the most stable conformations were chosen and optimized at the B3LYP/6-31G** + Δ ZPVE level of theory and also were computed at the B3LYP(PCM)/6-31G** + ZPVE level using water as solvent. Among them, the most stable of each compound was chosen to calculate the molecular DFT-based parameters, molecular electrostatic potential energetics and docking studies. The obtained results for the molecular electrostatic potential surfaces were generated using GaussView Rev 5.0.9 [31].

6.3.2. Docking studies

First, we proceeded with the choice of the most suitable TopIB/DNA complex for the docking in the Protein Data Bank (PDB). The X-ray structure code 1T8I [20] (3.00 Å resolution) was chosen, a TopIB of human origin covalently bounded to DNA and containing the anti-cancer agent CPT as a ligand. Maestro [23] graphic interface was used, and the Glide 6.9 application [32] in XP mode (extra-precision) [33] was chosen for the docking. The grid was set up in a box of 20 x 20 x 20 Å, centered in the geometric center of CPT. The DNA-binding region in the active site was selected as the target for the screening. The TopIB/DNA complex was prepared by reconstructing the phosphoester bond to nucleobase C12 in the 1T8I structure, and the 5'-SH of nucleobase G11 of the cleaved strand was converted to a 5'-OH by changing the sulfur atom by an oxygen. The hydrogen atoms were added. The binding orders and the protonation states of waste and DNA were corrected. The complex was optimized and minimized using the Protein Preparation Wizard panel of Schrödinger Suites 2015.1 [34]. Likewise, the structures of the different ligands to be interacted with protein and the ligand initially present in the complex, CPT, were prepared as previously indicated and used for the different docking processes.

Acknowledgements

Financial support from the *Ministerio de Ciencia, Innovación y Universidades (MCIU)*, *Agencia Estatal de Investigación (AEI)* y *Fondo Europeo de Desarrollo Regional (FEDER; RTI2018-101818-B-I00, UE)* and by *Gobierno Vasco, Universidad del País Vasco (GV, IT 992-16; UPV)* is gratefully acknowledged. Technical and human support provided by IZO-SGI, SGIker (UPV/EHU, MICINN, GV/EJ, ERDF and ESF) is gratefully acknowledged.

Corresponding Authors

*Phone: +34 945 013103; fax: +34 945 013049; e-mail: francisco.palacios@ehu.eus

*Phone: +34 945 013087; fax: +34 945 013049; e-mail: concepcion.alonso@ehu.eus

References

- [1] R. Siegel, D. Naishadham, A. Jemal, Cancer statistics. *Cancer J. Clin.* 63 (2013) 71–76.
- [2] Y. Pommier, C. Marchand, Interfacial inhibitors: targeting macromolecular complexes, *Nat. Rev. Drug Discov.* 11 (2012) 25–36 and references therein cited.
- [3] Y. Pommier, *Topoisomerases and cancer*. Springer: New York, 2012.
- [4] D C Gilbert, A J Chalmers, S F El-Khamisy, Topoisomerase I inhibition in colorectal cancer: biomarkers and therapeutic targets. *Br. J. Cancer.* 106 (2012) 18–24.
- [5] S. Antony, M. Jayaraman, G. Laco, G. Kohlhagen, K. W. Kohn, M. Cushman, Y. Pommier, Differential induction of topoisomerase I-DNA cleavage complexes by the indenoisoquinoline MJ-III-65 (NSC 706744) and Camptothecin: base sequence analysis and activity against Camptothecin-resistant Topoisomerases I. *Cancer Res.* 63 (2003) 7428–7435.
- [6] C. Alonso, E. Martín-Encinas, G. Rubiales, F. Palacios, Reliable synthesis of phosphino- and phosphine sulfide-1,2,3,4-tetrahydroquinolines and phosphine sulfide quinolones. *Eur. J. Org. Chem.* (2017) 2916–2924.
- [7] (a) A. Tejería, Y. Pérez-Pertejo, R. M. Reguera, R. Carbajo-Andrés, R. Balaña-Fouce, C. Alonso, E. Martín-Encinas, A. Selas, G. Rubiales, F. Palacios, Antileishmanial activity of new hybrid tetrahydroquinoline and quinoline derivatives with phosphorus substituents. *Eur. J. Med. Chem.* 162 (2019) 18–31. (b) C. Alonso, M. Fuertes, E. Martín-Encinas, A. Selas, G. Rubiales, C. Tesauro, B. R. Knudsen, F. Palacios, Novel topoisomerase I inhibitors. *Syntheses*

- and biological evaluation of phosphorus substituted quinoline derivatives with antiproliferative activity. *Eur. J. Med. Chem.* 149 (2018) 225–237.
- [8] A. Tejería, Y. Perez-Pertejo, R. M. Reguera, R. Balaña-Fouce, C. Alonso, M. González, G. Rubiales, F. Palacios, Substituted 1,5-naphthyridine derivatives as novel antileishmanial agents. Synthesis and biological evaluation. *Eur. J. Med. Chem.* 152 (2018) 137–147.
- [9] (a) M. B. Andersen, C. Tesauro, M. González, E. Kristoffersen, C. Alonso, G. Rubiales, A. Coletta, R. Froehlich, M. Stougaard, Y. Ho, F. Palacios, B. R. Knudsen, Advantages of an optical nanosensor system for mechanistic analysis of a novel topoisomerase I targeting drug: A case story. *Nanoscale* 9 (2017) 1886–1895. (b) A. Tejería, Y. Perez-Pertejo, R. M. Reguera, R. Balana-Fouce, C. Alonso, M. Fuertes, M. Gonzalez, G. Rubiales, F. Palacios, Antileishmanial effect of new indeno-1,5-naphthyridines, selective inhibitors of *Leishmania infantum* type IB DNA topoisomerase. *Eur. J. Med. Chem.* 124 (2016) 740–749. (c) C. Alonso, M. Fuertes, M. González, G. Rubiales, F. Palacios, Synthesis and biological evaluation of indeno[1,5]naphthyridines as topoisomerase I (TopI) inhibitors with antiproliferative activity. *Eur. J. Med. Chem.* 115 (2016) 179–190. (d) C. Alonso, M. Fuertes, M. González, G. Rubiales, A. Rodríguez-Gascón, G. Rubiales, F. Palacios, Synthesis and biological evaluation of 1,5-naphthyridines as topoisomerase I inhibitors. A new family of antiproliferative agents. *Curr. Topics Med. Chem.* 14 (2014) 2722–2728.
- [10] E. Martín-Encinas, G. Rubiales, B. R. Knudsen, F. Palacios, C. Alonso, Straightforward synthesis and biological evaluation as topoisomerase I inhibitors and antiproliferative agents of hybrid chromeno[4,3-*b*][1,5]naphthyridines and chromeno[4,3-*b*][1,5]naphthyridin-6(5*H*)-ones. *Eur. J. Med. Chem.* 178 (2019) 752–766.
- [11] K. M. Shea, in: J. J. Li (Ed.), *Name reactions for carbocyclic ring formations*, Wiley, Hoboken: NJ, 2010, pp. 275–308.
- [12]. S. Seghers, L. Protasova, S. Mullens, J. W. Thybaut, C. V. Stevens, Improving the efficiency of the Diels-Alder process by using flow chemistry and zeolite catalysis. *Green Chem.* 19 (2017) 237–248.
- [13] F. Palacios, C. Alonso, A. Arrieta, F. P. Cossío, J. M. Ezpeleta, M. Fuertes, G. Rubiales, Lewis Acid Activated Aza-Diels–Alder Reaction of *N*-(3-Pyridyl)aldimines: An Experimental and Computational Study. *Eur. J. Org. Chem.* (2010) 2091–2099.
- [14] O. Ghashghaei, C. Masdeu, C. Alonso, F. Palacios, R. Lavilla, Recent advances of the Povarov reaction in medicinal chemistry. *Drug Discov. Today* 29 (2018) 71–79.
- [15] S. Zou, K. L. Brown, Low temperature dehydrogenation of α -indoline nucleosides. *Tetrahedron Lett.* 45 (2004) 7783–7786.
- [16] (a) S. Castelli, A. Coletta, I. D’Annessa, P. Fiorani, C. Tesauro, A. Desideri T. Chandra, Interaction between natural compounds and human topoisomerase I. *Biol. Chem.* 393 (2012) 1327–1340. (b) P. Fiorani, G. Chillemi, C. Losasso, S. Castelli, A. Desideri, The different cleavage DNA sequence specificity explains the camptothecin resistance of the human topoisomerase I Glu418Lys mutant. *Nucleic Ac. Res.* 34 (2006) 5093–5100.
- [17] (a) T. Ziegler, Approximate density functional theory as a practical tool in molecular energetics and dynamics. *Chem. Rev.* 91 (1991) 651–667. (b) R. G. Parr, W. Yang, *Density-functional Theory of Atoms and Molecules*, Oxford University Press, Oxford, 1989.

- [18] (a) A. D. Becke, Density-functional exchange-energy approximation with correct asymptotic behaviour. *Phys. Rev. A* 38 (1998) 3098–3100. (b) W. Kohn, A. D. Becke, R. G. Parr, Density functional theory of electronic structure, *J. Phys. Chem.* 100 (1996) 12974–12980. (c) A. D. Becke, Density-functional thermochemistry. III. The role of exact exchange. *J. Chem. Phys.* 98 (1993) 5648–5652.
- [19] M. A. Bhat, S. H. Lone, M. A. Mir, S. A. Majid, H. M. Bhat, R. J. Butcher, S. K. Srivastava, Synthesis of t-butyl 2-(4-hydroxy-3-methoxybenzylidene) hydrazine carboxylate: experimental and theoretical investigations of its properties. *J. Mol. Struct.* 1164 (2018) 516–524 (and references therein cited).
- [20] B. L. Staker, M. D. Feese, M. Cushman, Y. Pommier, D. Zembower, L. Stewart, A. B. Burgin, Structures of Three Classes of Anticancer Agents Bound to the Human Topoisomerase I-DNA Covalent Complex, *J. Med.Chem.* 48 (2005) 2336–2345.
- [21] (a) N. M. Baker, R. Rajan, A. Mondragón, Structural studies of type I topoisomerases, *Nucleic Acids Res.* 37 (2009) 693–701. (b) D. A. Koster, K. Paile, E. S. M. Bot, M. A. Bjornsti, N. H. Dekker, Antitumour drugs impede DNA uncoiling by topoisomerase I, *Nature* 448 (2007) 213–217. (c) A. Lauria, M. Ippolito, A. M. Almerico, Molecular docking approach on the Topoisomerase I inhibitors series included in the NCI anti-cancer agents mechanism database, *J. Mol. Model.* 13 (2007) 393–400. (d) C. Marchand, S. Antony, K. W. Kohn, M. Cushman, A. Ioanoviciu, B. L. Staker, A. B. Burgin, L. Stewart, Y. Pommier, A novel norindenisoquinoline structure reveals a common interfacial inhibitor paradigm for ternary trapping of the topoisomerase I-DNA covalent complex, *Mol. Cancer Ther.* 5 (2006) 287–295.
- [22] G. Chillemi, L. Fiorami, P. Benedetti, A. Desideri, Protein concerted motions in the DNA-human topoisomerase I complex. *Nucleic Acids Res.* 31 (2003) 1525-1535.
- [23] Schrödinger Release 2015-1: Maestro, version 10.1, Schrödinger, L.L.C.: New York, 2015.
- [24] M. Lisby, B.O. Krogh, F. Boege, O. Westergaard, B.R. Knudsen, Camptothecins inhibit the utilization of hydrogen peroxide in the ligation step of topoisomerase I catalysis, *Biochemistry* 37 (1998) 10815–10827.
- [25] B. R. Knudsen, T. Straub, F. Boege, Separation and functional analysis of eukaryotic DNA topoisomerases by chromatography and electrophoresis, *J. Chromatogr. B: Biomed. Appl.* 684 (1996) 307-321.
- [26] Gaussian 16, Revision A.03, M. J. Frisch, G. W. Trucks, H. B. Schlegel, G. E. Scuseria, M. A. Robb, J. R. Cheeseman, G. Scalmani, V. Barone, G. A. Petersson, H. Nakatsuji, X. Li, M. Caricato, A. V. Marenich, J. Bloino, B. G. Janesko, R. Gomperts, B. Mennucci, H. P. Hratchian, J. V. Ortiz, A. F. Izmaylov, J. L. Sonnenberg, D. Williams-Young, F. Ding, F. Lipparini, F. Egidi, J. Goings, B. Peng, A. Petrone, T. Henderson, D. Ranasinghe, V. G. Zakrzewski, J. Gao, N. Rega, G. Zheng, W. Liang, M. Hada, M. Ehara, K. Toyota, R. Fukuda, J. Hasegawa, M. Ishida, T. Nakajima, Y. Honda, O. Kitao, H. Nakai, T. Vreven, K. Throssell, J. A. Montgomery, Jr., J. E. Peralta, F. Ogliaro, M. J. Bearpark, J. J. Heyd, E. N. Brothers, K. N. Kudin, V. N. Staroverov, T. A. Keith, R. Kobayashi, J. Normand, K. Raghavachari, A. P. Rendell, J. C. Burant, S. S. Iyengar, J. Tomasi, M. Cossi, J. M. Millam, M. Klene, C. Adamo, R. Cammi, J. W. Ochterski, R. L. Martin, K. Morokuma, O. Farkas, J. B. Foresman, and D. J. Fox, Gaussian, Inc., Wallingford CT, 2016.

- [27] J. W. Mciver Jr, A. J. Komornicki, Structure of transition states in organic reactions. General theory and an application to the cyclobutene-butadiene isomerization using a semiempirical molecular orbital method, *J. Am. Chem. Soc.* 94, (1972) 2625–2633.
- [28] (a) S. Miertus, E. Scrocco, J. J. Tomasi, Electrostatic interaction of a solute with a continuum. A direct utilization of AB initio molecular potentials for the prevision of solvent effects, *Chem. Phys.* 55, (1981) 117–129. (b) B. Mennucci, J. J. Tomasi, Continuum solvation models: A new approach to the problem of solute's charge distribution and cavity boundaries, *Chem. Phys.* 106, (1997) 5151–5158. (c) R. Cammi, B. Mennucci, J. J. Tomasi, Fast Evaluation of Geometries and Properties of Excited Molecules in Solution: A Tamm-Dancoff Model with Application to 4-Dimethylaminobenzonitrile, *Phys. Chem. A* 104 (2000) 5631–5637. (d) For an entry to the Polarized Continuum Model (PCM, solvent effects), see: J. Tomasi, B. Mennucci, R. Cammi, Quantum mechanical continuum solvation models, *Chem. Rev.* 105 (2005) 2999–3094.
- [29] Schrödinger Release 2015-1: Epik, version 3.1, Schrödinger, L.L.C.: New York, 2015.
- [30] Macro Model, Schrödinger, LLC, New York, NY 2018.
- [31] GaussView, Rev 5.0.9: R. Dennington, Todd A. Keith, and John M. Millam, Semichem Inc., Shawnee Mission, KS, 2016.
- [32] Schrödinger Release 2015-1: Glide, version 6.9, Schrödinger, L.L.C.: New York, 2015.
- [33] R. A. Friesner, R. B. Murphy, M. P. Repasky, L. L. Frye, J. R. Greenwood, T. A. Halgren, P. C. Sanschagrin, D. T. Mainz, Extra precision glide: docking and scoring incorporating a model of hydrophobic enclosure for protein-ligand complexes, *J. Med. Chem.* 49 (2006) 6177–6196.
- [34] Schrödinger Release 2015-1: Protein Preparation Wizard, Epik 3.1, Schrödinger, L.L.C.: New York, 2015.